Fundamentals of hypersonic flight - Properties of high temperature gases

P.F. Barbante *
Politecnico di Milano, Italy
T.E. Magin †
von Karman Institute for Fluid Dynamics, Belgium

Contents

*barbante@mate.polimi.it
†magin@vki.ac.be

Paper presented at the RTO AVT Lecture Series on "Critical Technologies for Hypersonic Vehicle Development", held at the von Kármán Institute, Rhode-St-Genèse, Belgium, 10-14 May, 2004, and published in RTO-EN-AVT-116.

1 Introduction

It is well known that a fluid, in the most general case, is made of a mixture of atoms and molecules. Air at ambient temperature, for example, is a mixture made of molecular nitrogen, molecular oxygen, plus a small percentage of argon, carbon dioxide, neon, and some other minor components. At moderate temperatures the gas behaves, with good approximation, as a *calorically perfect gas*. Gas pressure (p), density (ρ) and temperature (T) are linked by the well known and simple state law: $p = \rho RT$ (where R is the so called perfect gas specific constant). The gas specific heat are constant and internal energy and enthalpy are linear functions of the gas temperature. Also viscosity and thermal conductivity can be assumed to be constant, as a first approximation, or a simple power law dependence on temperature can be assumed.

When Mach number rises and temperature too, this simple picture no longer exists: new phenomena (so called *high temperature effects*) appear and the gas nature is drastically changed. We may grossly summarize such effects as follows:

- As temperature rises, the internal energy modes of the gas atoms and molecules, that at room temperature are dormant, are excited. Specific heats, internal energy and enthalpy are now nonlinear functions of the temperature. The specific heats ratio, also called γ, is no longer a constant. For air, excitation of the internal energy modes (vibrational) becomes important above temperatures of 500-800 K.

- As temperature further rises, chemical reactions can occur. Molecules dissociate into atoms, new molecules are eventually formed, atoms and molecules can ionize. Mixture thermodynamic and transport properties become functions not only of temperature but also of the chemical composition.

- Thermal nonequilibrium can also occur: internal energy modes are out of equilibrium with respect to the translational one; we can say that they do not "share" the same temperature. For example, when a fluid element crosses a shock wave, the translational energy of the fluid particles is suddenly increased; but a high number of collisions is needed to equilibrate the internal energy modes with the translational one (Park, 1990). Therefore, behind the shock, there will be a relaxation region where the internal energy modes will try to "catch up" the translational one. Another example is when the fluid experiences a strong expansion. In this case the translational energy will rapidly decrease because of the expansion, but the internal one will remain higher.

- Ionization can occur and the gas becomes a partially ionized plasma, with a finite electrical conductivity. Therefore electromagnetic fields and associated forces, either self-induced or applied from an external source (Peterkin and Turchi, 2000; Sutton and Sherman, 1965), can act on the fluid, appreciably changing its behaviour with respect to a neutral one. To make things more complex, an additional source of thermal nonequilibrium appears because energy exchange between mixture components and free electrons is highly inefficient due to the large mass disparity: in this case the translational temperature of electrons can be different from the one of heavy particles (Park, 1990).

- At high temperature (above 10000-11000 K for air) radiation emitted and absorbed by the gas can become important (Park, 1990) and eventually modify the energy distribution in the flowfield. Radiation modeling is a formidable task (Park, 1990; Sarma, 2000; Vincenti and Kruger, 1965), both numerically (a fluid element, a priori, is influenced by and influences all the others) and physically (an adequate spectral data base is required).

- Chemical reactions can take place not only in the bulk of the gas but also at the surface of the vehicle, due to catalytic effects of the wall material upon surface chemistry. Usually such reactions have the negative property of increasing the heat flux experienced by the vehicle (Nasuti et al., 1996; Sarma, 2000).

We present now in a very qualitative manner two practical cases where high temperature gases showing some, if not all, of the previously described effects are encountered.

High speed vehicles

It is well known that, when an aerospace vehicle travels at high speed through the atmosphere, a strong shock is formed in front of it. A major part of the kinetic energy of the free stream flow is converted into thermal energy across the shock and therefore high temperature is reached in the flow region between the shock and the body (the shock layer). The intense friction happening in the boundary layer increases too the temperature triggering further chemical reactions. The high temperature effects can have a strong impact on boundary layer stability and transition to turbulence. When the shock layer temperature is high enough the gas can ionize: the free electrons absorb radio waves and cause communication blackout to and from the vehicle. This is a serious problem and an accurate prediction of the electron number density in the shock layer is important. Emission and absorption of radiation can occur and, besides affecting the state of the gas surrounding the vehicle, can raise the heat flux experienced by the vehicle itself. Radiation from the hot vehicle wall to the ambient atmosphere can have a significant cooling effect and must be taken into account in the thermal boundary condition (Sarma, 2000).

Ramjet and Scramjet engines

A Ramjet engine is essentially a duct where supersonic air is slowed down to subsonic speed at the entrance of the combustor. Fuel is injected in the combustor, the mixture burns and expands through the nozzle. Ramjets have advantages over conventional turbine engines in the Mach number regime from 2 to 5. However, some design concepts of hypersonic airbreathing transport vehicles assume a flight Mach number well in excess of 10 (an example being the NASA X-43A). Under such conditions, if the incoming air is decelerated to subsonic speed, it attains a temperature that is above the adiabatic flame temperature of the fuel-air mixture burning in the combustor and therefore no combustion can take place. A possible solution is to keep the incoming air stream at supersonic speed in the combustor: in this way air temperature is kept below the flame adiabatic temperature and combustion can take place. The major drawback is that the combustion has to take place in a supersonic stream, leading to tremendous practical problems (flame stabilization, efficient mixing and burning) that are still not solved nowadays.

Lecture layout

In Sec. 2 we will recall the governing equations for a mixture of gases under conditions of chemical nonequilibrium but thermal equilibrium. In Sec. 3 the thermodynamic properties of each mixture component will be given. In Sec. 4 a short discussion of chemistry and wall catalycity phenomena will be provided. Finally in Sec. 5 transport fluxes and related transport coefficients will be discussed. Some examples of computations of high temperature reacting flows will be provided in Sec. 6.

2 Governing Equations

The governing equations are the mathematical expression of the physical principles of conservation of mass, momentum and energy. They can be derived, for example, with the control volume method, which is very general, not linked with a specific physico-chemical model and therefore does not give the expression of all the terms in the governing equations. The missing terms are provided by statistical mechanics and kinetic theory. Statistical mechanics provides the thermodynamic properties (internal energy, specific heat) and kinetic theory provides the transport properties (viscosity, thermal conductivity, diffusion).

High temperature fluids are in general made of different chemical species; in the range of pressure and temperature of interest here, each one behaves with good approximation as a perfect gas. We make the key assumption that the gas can be described as a continuum, i.e. there are always a sufficient number of molecules within the smallest significant volume of the fluid and the macroscopic properties are given by average values of the appropriate molecular quantities. We also assume that the gradients of the macroscopic variables (e.g. density, speed, temperature) have a characteristic length L that is much bigger than the mean free path λ. Defining the Knudsen number as: $Kn = \lambda/L$, the previous assumption corresponds to: $Kn \ll 1$. The governing equations of such flows are the Navier-Stokes ones and the transport terms (shear stresses, heat flux, diffusion fluxes) can be expressed as functions of macroscopic quantities (e.g. density, velocity, temperature, pressure). It is the failure to meet this condition which imposes a limit in the continuum equations. The Navier-Stokes equations tend to become inapplicable for $Kn > 0.03$, and even when they are approximately applicable, the usual no-slip boundary conditions are not any more valid. More specifically, the relative flow velocity at a surface, which is usually assumed to be zero, takes a finite value: this is called the slip velocity condition. In a similar fashion, the temperature, which is usually taken equal to the surface temperature, now becomes different: it is the temperature slip condition. A way to fix such a behaviour is to use slip boundary conditions with the Navier-Stokes equations, an approach that has been proven to be quite effective (Gupta, 1996a,b) and gives good results up to $Kn = 0.1$. The error in the Navier-Stokes results is significant in regions of the flow where $Kn > 0.1$ and the continuum model has to be replaced by the molecular model for $Kn > 0.2$. As already stated, the discussion presented in this lecture is valid in the continuous regime and the slip effects are negligible.

2.1 Continuity equation

This equation simply expresses the conservation of global mass in the system. In Eulerian differential form is written as:

$$\frac{\partial \rho}{\partial t} + \nabla \cdot (\rho \vec{v}) = 0 \tag{1}$$

where ρ is the mixture density and $\vec{v}$ is the mixture average velocity. If ρ_i is the partial density of each mixture component, we have: $\rho = \sum_{i=1}^{N_S} \rho_i$, where N_S is the number of mixture chemical species. If $\vec{v}_i$ is the average velocity of each mixture component, then $\vec{v}$

is defined as:

$$\vec{v} = \frac{\sum_{i=1}^{N_S} \rho_i \vec{v}_i}{\rho} \tag{2}$$

2.2 Species continuity equation

The appropriate equations for each of the components must be established to compute the mixture chemical composition. Partial densities are a natural choice and the species continuity equations are then:

$$\frac{\partial \rho_i}{\partial t} + \nabla \cdot (\rho_i \vec{v}_i) = \dot{w}_i \tag{3}$$

where $\dot{w}_i$ is the chemical production term, i.e. the term that accounts for the rate of production or depletion of species i due to chemical reactions. The average velocity for species i, $\vec{v}_i$, can be written as:

$$\vec{v}_i = \vec{v} + \vec{V}_i \tag{4}$$

where $\vec{V}_i$ is the diffusion velocity for species i. A related term is:

$$\vec{J}_i = \rho_i \vec{V}_i \tag{5}$$

which is the diffusion flux and it plays a very important role in the framework of reacting flows. Naturally, summing up all the species continuity equations, we have to recover the global continuity equation. Indeed we have: $\sum_{i=1}^{N_S} \rho_i = \rho$; and the chemical production terms satisfy the property $\sum_{i=1}^{N_S} \dot{w}_i = 0$. From Eq. (2) and (4) we can deduce an important property of diffusion fluxes:

$$\sum_{i=1}^{N_S} \vec{J}_i = \sum_{i=1}^{N_S} \rho_i \vec{V}_i = 0 \tag{6}$$

This taken into account we rewrite Eq. (3) under the form:

$$\frac{\partial \rho_i}{\partial t} + \nabla \cdot \left(\rho_i \vec{v} + \vec{J}_i \right) = \dot{w}_i \tag{7}$$

2.3 Momentum equation

The momentum conservation equation can be written:

$$\frac{\partial \rho \vec{v}}{\partial t} + \nabla \cdot (\rho \vec{v} \otimes \vec{v}) + \nabla p = \nabla \cdot \bar{\bar{\tau}} + \sum_{i=1}^{N_S} \rho_i \left(\vec{F}_{gi} + \vec{F}_{ei} \right) \tag{8}$$

where p is the mixture pressure, $\bar{\bar{\tau}}$ is the viscous stress tensor, $\vec{F}_{gi}$ is a nonelectromagnetic body force and $\vec{F}_{ei}$ is the electromagnetic force, both acting on the species i. If the species i is neutral the electromagnetic force is zero. $\vec{F}_{gi}$ reduces in the applications presented here to gravity and is always neglected; this is justified because in our applications the buoyancy effects are negligible. $\vec{F}_{ei}$ arises because of the presence of electromagnetic fields and has the form:

$$\vec{F}_{ei} = \frac{q_i}{m_i} \left(\vec{E} + \vec{V}_i \times \vec{B} \right) \tag{9}$$

where m_i is the mass of particle i and q_i its charge. In the above equation, $\vec{E}$ is the electric field and $\vec{B}$ the induced magnetic field. Usually Maxwell equations are needed to compute the electric field and the induced magnetic field (Sutton and Sherman, 1965). In the presence of a ionized mixture, when no external fields are applied one can suppose that the magnetic field is negligible and the electric field is computed from the ambipolar constraint, i.e. the diffusion current is zero in the flow:

$$\sum_{i=1}^{N_S} q_i x_i \vec{V_i} = 0 \tag{10}$$

where x_i is the molar fraction.

2.4 Energy equation

In compressible flows it is important to take into account both internal and kinetic energy in the energy equation, because there is a strong coupling between the two, through conversion of one energy type into the other (as, for example, across a shock, where kinetic energy is converted into thermal energy).

The total energy conservation equation for the mixture is:

$$\frac{\partial \rho E}{\partial t} + \nabla \cdot \left[(\rho E + p)\, \vec{v} \right] - \nabla \cdot (\bar{\bar{\tau}} \cdot \vec{v}) + \nabla \cdot \vec{q} = \sum_{i=1}^{N_S} \left(\rho_i \vec{v} + \rho_i \vec{V_i} \right) \cdot \left(\vec{F}_{gi} + \vec{F}_{ei} \right) \tag{11}$$

where E is the total energy (per unit mass) i.e. the sum of the mixture internal and kinetic energy: $E = e + v^2/2$. The third term in the left hand side is the work of the viscous stresses, the fourth the heat flux, the term on the right hand side is the work of the body forces.

2.5 Mixture parameters and perfect gas law

The thermodynamic state of a mixture of perfect gases is uniquely defined once the temperature T, the pressure or the density and the chemical composition are specified. For most problems in aerodynamics it is indeed reasonable to assume that each species is a perfect gas. Conditions that violates this assumptions are very high pressure ($p > 1000\, bar$) or low temperature ($T < 30\, K$), both of which are far from the typical conditions met in aerospace applications. For each mixture component the equation of state linking temperature T and partial density ρ_i and pressure p is:

$$p_i = \rho_i R_i T \tag{12}$$

R_i is the specific gas constant that may also be expressed as:

$$R_i = \frac{\mathcal{R}}{M_i} \tag{13}$$

$\mathcal{R}$ is the universal gas constant, which is the same for all species (at least if they behave as a perfect gas), M_i is the species molar mass, i.e. the mass of a mole of the species.

Dalton's law for perfect gases states that the mixture pressure p is equal to the sum of the species partial pressures p_i:

$$p = \sum_{i=1}^{N_S} p_i \tag{14}$$

The same law is valid for the partial densities ρ_i:

$$\rho = \sum_{i=1}^{N_S} \rho_i \tag{15}$$

where ρ is, by definition, the mixture density. From Dalton's law (Eq. 14) we infer that once the temperature and the partial pressures p_i of each component are known, the mixture is completely specified.

Other quantities are suited to describe the mixture chemical composition:

- The mass fractions $y_i = \frac{\rho_i}{\rho}$ (mass of species i per unit mass of mixture).
- The mole fractions x_i (number of moles of species i per mole of mixture);

Both quantities satisfy the condition:

$$\sum_{i=1}^{N_S} y_i = \sum_{i=1}^{N_S} x_i = 1$$

Mole and mass fractions can be used to compute mixture molar mass (M) and specific gas constant (R) respectively:

$$\sum_{i=1}^{N_S} y_i R_i = R \tag{16}$$

$$\sum_{i=1}^{N_S} x_i M_i = M \tag{17}$$

The formula to convert mole fractions into mass fractions (and vice versa) is:

$$y_i = \frac{M_i}{M} x_i \tag{18}$$

When using mole fractions one has to remember that the total number of moles in the system does change due to chemical reactions; the total mass, however, remains unchanged.

3 Thermodynamic properties

3.1 Energy, enthalpy, specific heat

Atoms and molecules have different modes to store energy and each mode is quantized, i.e. it can only take discrete values (Anderson, 1989; Mayer and Mayer, 1946). In an atom there are two energy modes:

- Translational energy mode: associated with the motion of centre of mass;
- Electronic energy mode: associated with the electrons orbiting around the nucleus.

For a molecule there are additional energy modes:

- Rotational energy mode: associated with the rotation of the molecule around orthogonal axes in space;
- Vibrational energy mode: associated with the vibration of the atoms of the molecule with respect to equilibrium positions within the molecule.

Every energy mode can assume an ensemble of, in theory infinite, different discrete values, or levels. Each level, in its turn, may manifest itself in a number of different ways (degeneracy, g_i^k, of the levels).

For a system of N_i particles of species i, distributed among an ensemble of k energy levels, each of them with a different energy content, ϵ_i^k, the total energy E_i is:

$$E_i = \sum_{k=0}^{\infty} \epsilon_i^k N_i^k \tag{19}$$

(with the constraint $\sum_{k=0}^{\infty} N_i^k = N_i$). Every distinguishable arrangement of the N_i particles among the levels is a macrostate. A way of computing the possible macrostates is to set up a differential equation for each level, an exceedingly complex task. To avoid such a task one can look for the existence of a macrostate that is much more likely to occur than any other. Indeed such a state does exists, it is called the most probable macrostate (or the most probable distribution), its probability is overwhelmingly higher than the one of other possible macrostates (Vincenti and Kruger, 1965) and it occurs when the system is in thermodynamic equilibrium. The latter is a very important point because it restricts the use of the most probable macrostate to conditions of *thermodynamic equilibrium or of slight nonequilibrium*. The distribution of the particles over the different levels for the most probable macrostate is given by:

$$N_i^k = N_i \frac{g_i^k \exp\left(-\frac{\epsilon_i^k}{k_B T}\right)}{Q_i} \tag{20}$$

(k_B being the Boltzmann constant). The quantity Q_i is the system partition function and is given by:

$$Q_i = \sum_{k=0}^{\infty} g_i^k \exp\left(-\frac{\epsilon_i^k}{k_B T}\right) \tag{21}$$

The power of the partition function lies in the fact that the thermodynamic properties of the system can be determined from the partition function itself (Anderson, 1989; Clarke and McChesney, 1964; Vincenti and Kruger, 1965). For example, the internal energy per unit mass of species i is given by:

$$e_i = R_i T^2 \frac{\partial \ln Q_i}{\partial T} \tag{22}$$

Once the expression for the energy content ϵ_i^k of the different quantum states is known, the partition function can be computed by means of Eq. 21 and the internal energy is finally evaluated from Eq. 22. It is customary to express the level energies, ϵ_i^k, relative to the value they assume at absolute zero (also called the zero-point energy or ground state), so that the computed energy is not the absolute energy but instead the sensible one. The total energy is thus obtained by addition of the zero point energy $e_{0,i}$.

For perfect gases the translational and the internal modes are independent of each other and the partition function can be factored into two separate contributions: $Q = Q_T Q_{int}$ (where Q_{int} belongs to the internal modes). In a real molecule the internal energy modes are not truly independent of each other: the energy content of an internal mode is affected by the state of the other internal modes (Mayer and Mayer, 1946). Therefore, when computing Q_{int}, the contribution of a single mode cannot be factored separately from the others. However, for the simplest molecule model, which is the rigid rotator-harmonic oscillator, the rotational, vibrational and electronic energy modes are considered to be independent each other and the molecular partition function can be factored as: $Q = Q_T Q_R Q_V Q_E$. (Subscript T refers to translation mode, R to rotational, V to vibrational and E to electronic).

In agreement with the factorization property of the partition function, the internal energy for an atom can be written as:

$$e_i = e_{T,i} + e_{E,i} + e_{0,i}$$

For a molecule the internal energy is:

$$e_i = e_{T,i} + e_{int,i} + e_{0,i}$$

Or, if all the internal modes are independent:

$$e_{int,i} = e_{R,i} + e_{V,i} + e_{E,i}$$

The translational energy is the same for both atoms and molecules and its value per unit mass is:

$$e_{T,i} = \frac{3}{2} R_i T \tag{23}$$

The electronic energy for atoms (and also for molecules when it can be factored) has no simple expression and reads (per unit mass):

$$e_{E,i} = R_i \frac{\sum_{k=0}^{\infty} g_{Ei}^k \theta_{E,i}^k \exp\left(\frac{-\theta_{E,i}^k}{T}\right)}{\sum_{k=0}^{\infty} g_{Ei}^k \exp\left(\frac{-\theta_{E,i}^k}{T}\right)} \tag{24}$$

g^k_{Ei} is the degeneracy for level k, $\theta^k_{E,i}$ is the characteristic electronic temperature for level k. The series in Eq. 24 diverges and has to be truncated. An empirical but effective criteria is to take into account the strictly necessary minimum number of electronic levels that produce a non-negligible change of energy in the temperature range of interest (Bottin et al., 1999).

For a linear molecule behaving as a rigid rotator-harmonic oscillator, the rotational energy per unit mass can be written as:

$$e_{R,i} = R_i T \left(1 - \frac{\theta_{R,i}}{\theta_{R,i} + 3T}\right) \tag{25}$$

$\theta_{R,i}$ is the rotational characteristic temperature and is usually equal to a few Kelvin, so that the rotational mode is fully excited at temperatures considered here. The vibrational energy per unit mass is, in its turn:

$$e_{V,i} = R_i \sum_m \frac{\theta^m_{V,i}}{\exp\left(\frac{\theta^m_{V,i}}{T}\right) - 1} \tag{26}$$

$\theta^m_{V,i}$ is the vibrational characteristic temperature associated with the vibrational mode m. The vibrational energy contribution is less than $R_i T$ and approaches this value when $T \gg \theta^m_{V,i}$.

The zero-point energy generally cannot be computed or measured; nevertheless it is an important quantity. In a reacting mixture it is necessary to establish a common level from which all the species energies are measured. In addition the zero-point energy is linked with the energy associated with chemical bonds. Consider for example a certain amount of nitrogen atoms; it is experimentally observed that, when they recombine to form molecular nitrogen, some energy is released. If the recombination happens at the absolute zero, the energy released in the chemical reaction (Δh^0_F) is equal to the difference between the zero-point energy of the atomic nitrogen mixture $e_{0,N}$ and of the molecular nitrogen mixture e_{0,N_2}. If the reaction proceeds in the opposite direction, exactly the same amount of energy is absorbed by the system: it is the heat of formation of atomic nitrogen at absolute zero. From the point of view of the energy balance it is equivalent to assume $e_{0,N} \neq 0$, $e_{0,N_2} \neq 0$ and $\Delta h^0_F = e_{0,N} - e_{0,N_2}$ or $e_{0,N} = \Delta h^0_F$, $e_{0,N_2} = 0$ and obviously $\Delta h^0_F = e_{0,N} - e_{0,N_2}$. Therefore it follows that the zero-point energy $e_{0,i}$ of species i can be replaced by the heat of formation $\Delta h^0_{F,i}$ of species i at the same temperature. The heat of formation of the different species is available in literature (Chase et al., 1985).

The enthalpy is simply computed from the energy by addition of the extra term: $R_i T$.

As previously mentioned, the rigid rotator-harmonic oscillator model for the molecules does not truly represent the reality and so-called anharmonicity corrections can be used (Bottin et al., 1999): they take into account the fact that the energy modes are coupled together. Anharmonicity corrections often change appreciably the molecules internal energy. It should be noticed, however, that this effect is more pronounced above $6000\,K$, a temperature at which, usually, molecules are highly dissociated. The correction has a small effect on the mixture properties and can often be neglected.

The mixture energy and enthalpy per unit mass are obtained by means of the formulae:

$$e = \sum_{i=1}^{N_S} y_i e_i \qquad\qquad h = \sum_{i=1}^{N_S} y_i h_i \tag{27}$$

Enthalpy of Local Thermodynamic Equilibrium (LTE) air is shown in Fig. 1.

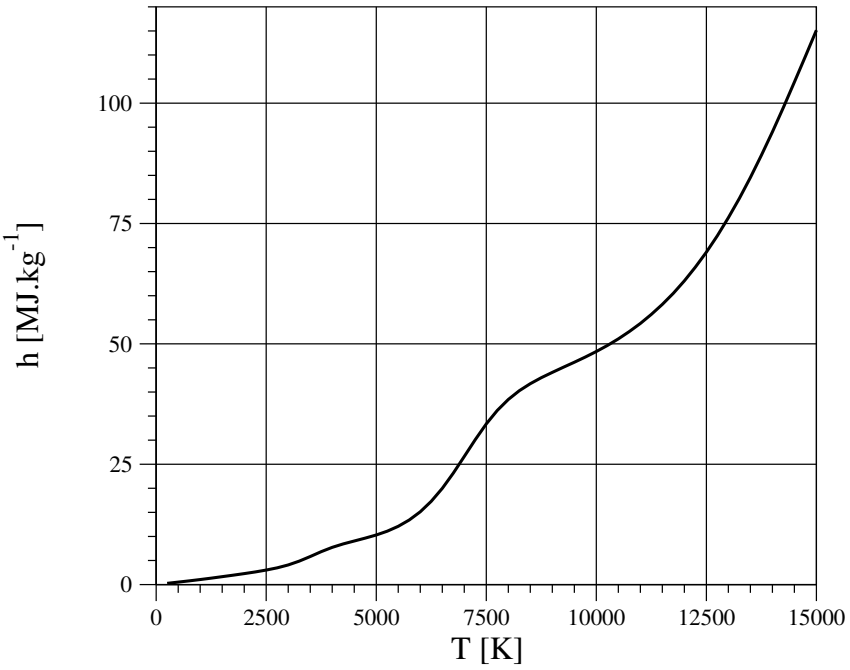

Figure 1: Enthalpy of air at 1 *atm*.

Enthalpy of LTE carbon dioxide is given in Fig. 2. The negative value of enthalpy at low temperature results of the exothermic formation of the CO_2 molecule at 0 K (the enthalpy of formation of carbon graphite and molecular oxygen gas is zero).

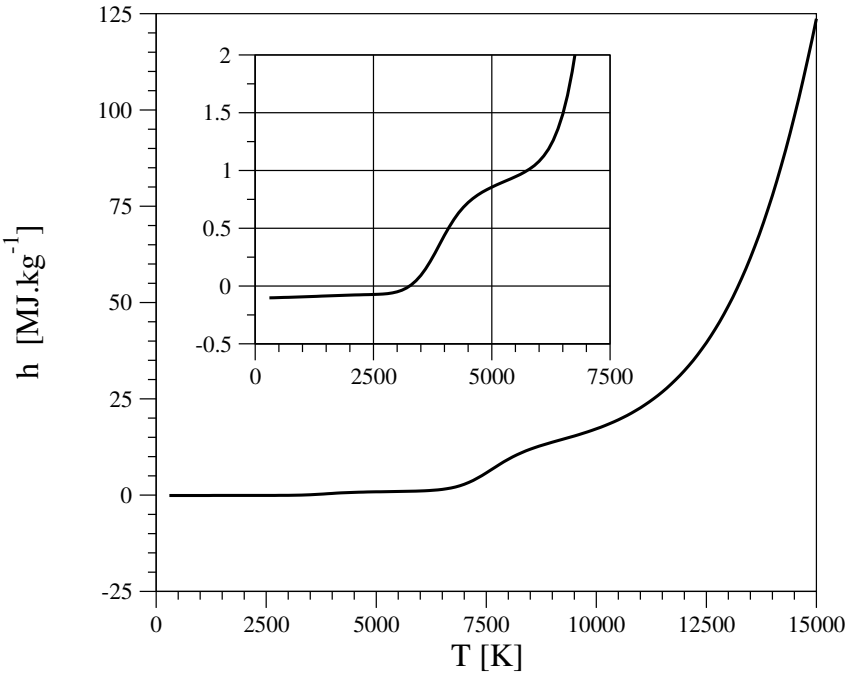

Figure 2: Enthalpy of carbon dioxide at 1 *atm*.

The single species specific heats are, by definition:

$$c_{v,i} = \left(\frac{\partial e_i}{\partial T}\right)_v \qquad c_{p,i} = \left(\frac{\partial h_i}{\partial T}\right)_p \tag{28}$$

Both are functions of temperature only, as it is the case for the internal energy and the enthalpy.

The specific heat for a mixture requires a little bit more care. Let's concentrate on the constant pressure specific heat c_p, the same being valid for c_v. From Eq. 27 and 28 we have:

$$c_p = \left(\frac{\partial h}{\partial T}\right)_p = \sum_{i=1}^{N_S} \left[\left(\frac{\partial y_i}{\partial T}\right)_p h_i + y_i \left(\frac{\partial h_i}{\partial T}\right)_p\right] \tag{29}$$

If no chemical reactions are taking place in the flow (the mixture is frozen) the first derivative is identically zero and we have the frozen specific heat:

$$c_{p,fr} = \sum_{i=1}^{N_S} y_i \left(\frac{\partial h_i}{\partial T}\right)_p = \sum_{i=1}^{N_S} y_i c_{p,i} \tag{30}$$

In case of a frozen mixture, chemical composition does not change (y_i is constant) and $c_{p,fr}$ is function only of temperature: *a frozen mixture is therefore a thermally perfect gas.* If, on the opposite, chemical equilibrium is established, the chemical composition is function only of two thermodynamic variables, e.g. pressure and temperature or, $y_i = y_i(p, T)$ and Eq. 28 becomes:

$$c_{p,eq} = \sum_{i=1}^{N_S} \left[\left(\frac{\partial y_i}{\partial T}\right)_p h_i + y_i c_{p,i}\right] \tag{31}$$

In the intermediate case of a finite rate chemically reacting mixture, the chemical composition is function not only of two thermodynamic variables, but also of the position and of the previous flow history. It follows that the derivative $\left(\frac{\partial y_i}{\partial T}\right)_p$ is not uniquely defined and the only kind of specific heat that makes sense is the frozen specific heat $c_{p,fr}$ given by Eq. 30.

Frozen and equilibrium specific heat of LTE air are shown in Fig. 3. Frozen and equilibrium specific heat of LTE carbon dioxide are shown in Fig. 4.

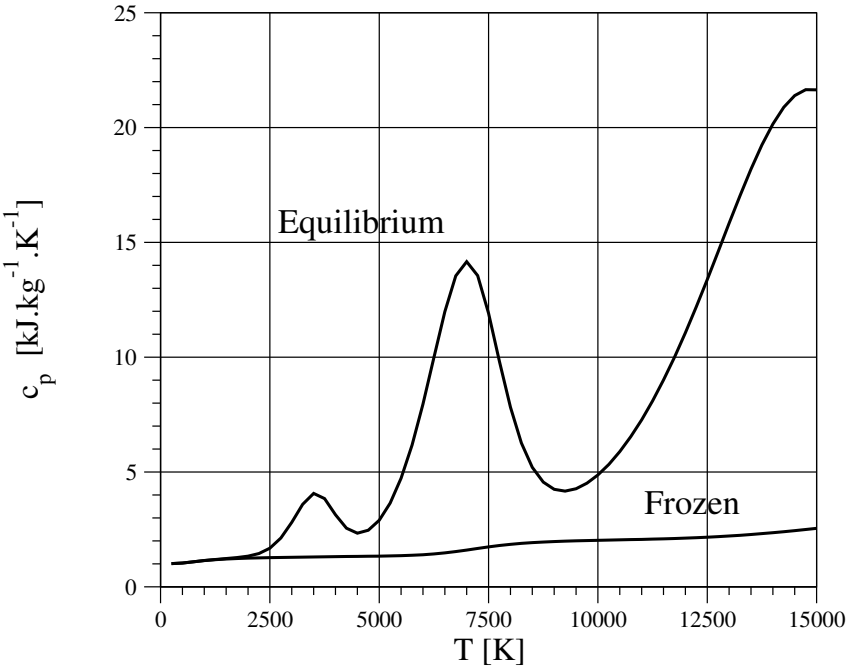

Figure 3: Specific heat of air at 1 *atm*.

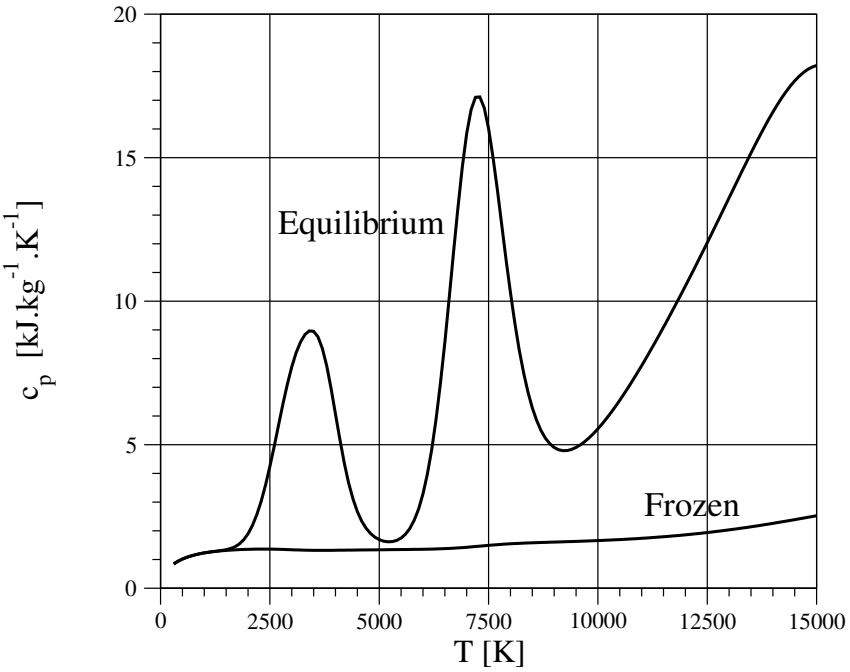

Figure 4: Specific heat of carbon dioxide at 1 *atm*.

3.2 Speed of sound

The speed of sound is by definition:

$$c^2 = \left(\frac{\partial p}{\partial \rho}\right)_s \tag{32}$$

i.e. the derivative of pressure with respect to density at constant entropy. As for the specific heats we can define two different speeds of sound (Anderson, 1989; Clarke and McChesney, 1964): a frozen speed of sound c_{fr} and an equilibrium speed of sound c_{eq}. The frozen sound speed is:

$$c_{fr}^2 = \frac{c_{p,fr}}{c_{v,fr}} \frac{p}{\rho} = \gamma_{fr} \frac{p}{\rho} = \gamma_{fr} RT \tag{33}$$

The equilibrium speed of sound is:

$$c_{eq}^2 = \frac{c_{p,eq}}{c_{v,eq}} \frac{p}{\rho} \frac{1 - \frac{\rho^2}{p} \left(\frac{\partial e}{\partial \rho}\right)_T}{1 - \rho \left(\frac{\partial h}{\partial p}\right)_T} = \frac{c_{p,eq}}{c_{v,eq}} \frac{1}{\left(\frac{\partial \rho}{\partial p}\right)_T} \tag{34}$$

When the flow is either frozen or in chemical equilibrium, there is no ambiguity on which sound speed has to be used. In case of chemical nonequilibrium, disturbances with a period (the inverse of the frequency) much longer than the characteristic time of the chemistry propagate with the equilibrium sound speed, disturbances with a period much smaller than the chemistry time with the frozen sound speed and disturbances with a period of the same order as the chemistry time propagate with an intermediate speed (Clarke and McChesney, 1964). This creates problems for the choice of the speed to use in a chemically reacting flow computation.

The frozen and equilibrium sound speed are given in Fig. 5 for LTE air.

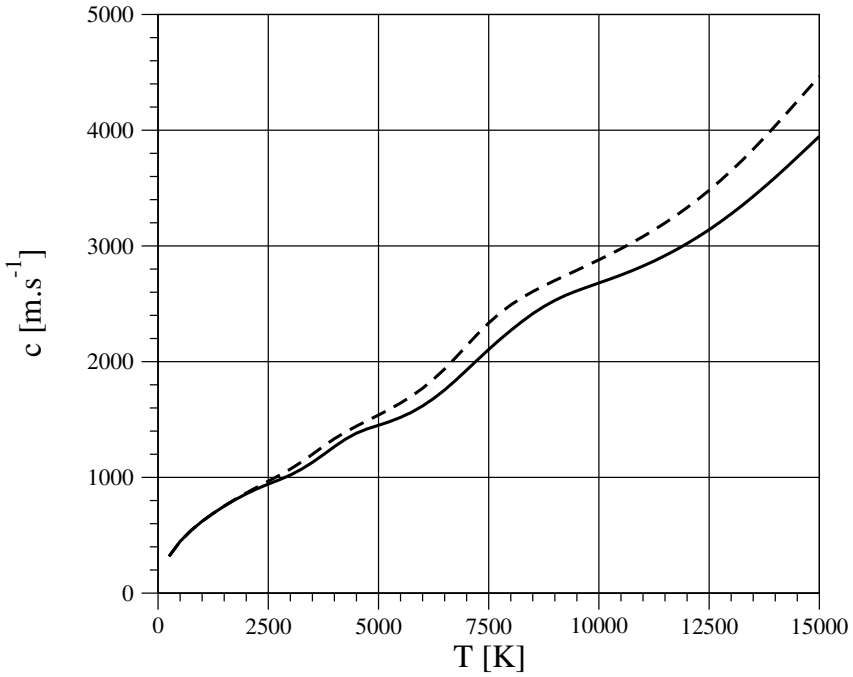

Figure 5: Sound speed of air at 1 *atm*: –– frozen and — equilibrium.

The equilibrium speed of sound is compared in Fig. 6 to the frozen speed of sound for LTE carbon dioxide.

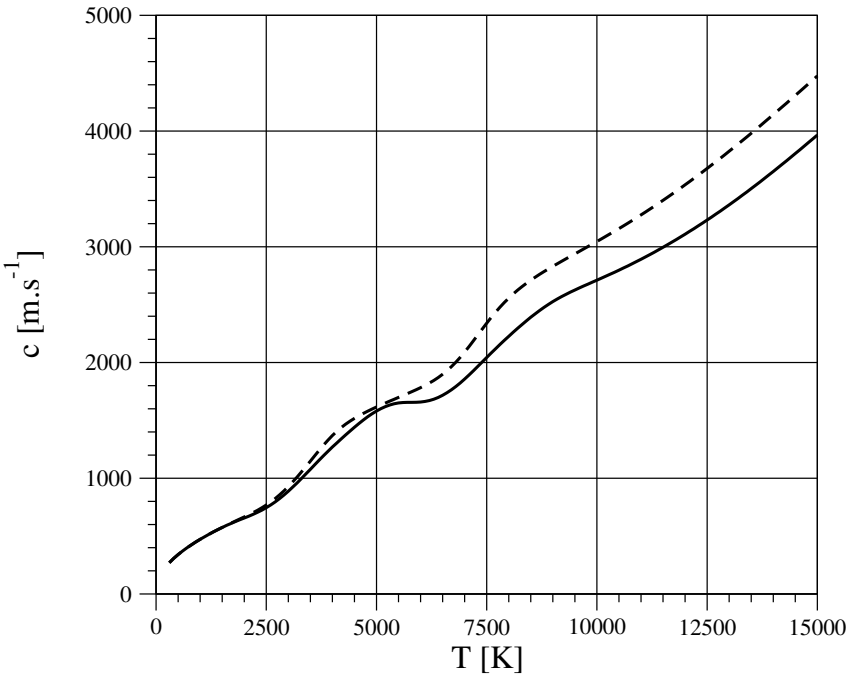

Figure 6: Sound speed of carbon dioxide at 1 atm: −− frozen and — equilibrium.

4 Chemistry

4.1 Equilibrium chemistry

Let's now recall the species i continuity equation (Eq. 3) and let's put aside, for the moment, the convective and diffusive terms. The equation reduces to the ordinary differential equation (ODE) $\frac{\partial \rho_i}{\partial t} = \dot{w}_i$. Adding all the species we have a system of ODE's governing the evolution of the N_S species. The system is, in general, nonlinear because of the structure of the production term (Eq. 38). In a first approximation we can linearize the system around a known state ρ_i^0.

$$\frac{\partial \rho_i}{\partial t} = \dot{w}_i^0 + \sum_{j=1}^{N_S} \frac{\partial \dot{w}_i}{\partial \rho_j}(\rho_j - \rho_j^0) = \overline{\dot{w}}_i^0 + \sum_{j=1}^{N_S} \frac{\partial \dot{w}_i}{\partial \rho_j}\rho_j \qquad i = 1, \ldots, N_S$$

or, in compact form:

$$\frac{\partial}{\partial t}\{\rho_i\} = \left\{\overline{\dot{w}}_i^0\right\} + [A]\{\rho_i\}$$

$\dot{w}_i$ has dimensions $kg/(m^3 s)$ and thus each element of the Jacobian $[A]$ has dimensions $1/s$ and is an index of the characteristic time of chemical reactions. The element $\partial \dot{w}_i/\partial \rho_j$ may also be seen as the sensitivity, due to chemical reactions, of species i with respect to a variation of species j. For practical purposes, we can think of having only a global value for the characteristic time of chemical reactions, instead of the N_S by N_S given by the Jacobian. The norm of $[A]$ ($|||[A]|||$) is taken as the desired value.

The next step is to compare a characteristic flow time (e.g. the time that the flow needs to cross the region of interest) with the chemistry time. In order to do this the species continuity equation (Eq. 3) is conveniently non-dimensionalised. We define a reference length L_{ref}, a reference speed v_{ref}, a reference density ρ_{ref} and a reference chemistry time $1/\tau_c = |||[A]|||_{ref}$, the flow reference time being defined as $\tau_f = L_{ref}/v_{ref}$. The species equation in nondimensional form reads:

$$\frac{\partial \tilde{\rho}_i}{\partial \tilde{t}} + \tilde{\nabla} \cdot \left(\tilde{\rho}_i \tilde{\vec{v}}_i\right) = \tilde{\dot{w}}_i |||[A]|||_{ref} \frac{L_{ref}}{v_{ref}} = Da_1 \tilde{\dot{w}}_i \tag{35}$$

(where the $\tilde{}$ superscript indicates a nondimensional quantity). The quantity $Da_1 = \tau_f/\tau_c$ is the first Damköhler number and it is a parameter of fundamental importance in the study of similitude in reacting flows. By analyzing the previous equation we can define the two following limiting cases:

- If $\tau_f \ll \tau_c$ or $Da_1 \to 0$, the chemical reactions are negligible, the flow is called frozen flow and the species continuity equations reduce to:

$$\frac{\partial \rho_i}{\partial t} + \nabla \cdot (\rho_i \vec{v}_i) = 0$$

- If $\tau_f \gg \tau_c$ or $Da_1 \to \infty$, the flow tends towards a state of local chemical equilibrium and the species continuity equations tend to the limit

$$\dot{w}_i = 0$$

In this case the chemical composition is uniquely determined by the local values of p and T or ρ and T. The species continuity equations may be eliminated from the system of governing equations and the chemical composition computed with an ad hoc algorithm (Bottin et al., 1999; Anderson, 1989).

The computed equilibrium composition of air for Earth reentries and carbon dioxide for Mars entries is shown in Figs. 7 and 8. The mixtures are defined as follows:

- An 11-species air mixture composed of N_2, NO, O_2, N, O, N_2^+, NO^+, N^+, O_2^+, O^+, and e^-, with 79 % of nitrogen and 21 % of oxygen elements.
- An 8-species carbon dioxide mixture composed of CO, CO_2, O_2, C, O, C^+, O^+ and e^-, with 1/3 of carbon and 2/3 of oxygen elements.

The net charge is zero.

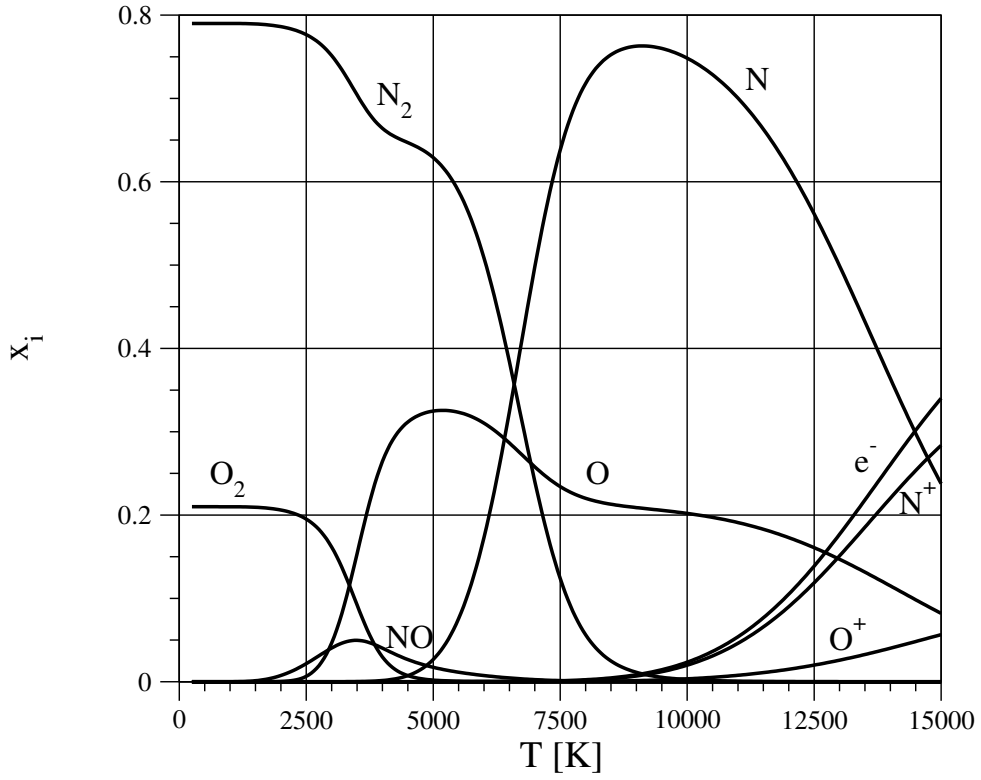

Figure 7: Major components of air at 1 atm.

4.2 Nonequilibrium chemistry

We begin by considering an elementary reaction (identified with index r), i.e. a reaction accomplished in one step only, which can be formally written as:

$$\sum_{i=1}^{N_S} \nu'_{ir} X_i \rightleftarrows \sum_{i=1}^{N_S} \nu''_{ir} X_i \tag{36}$$

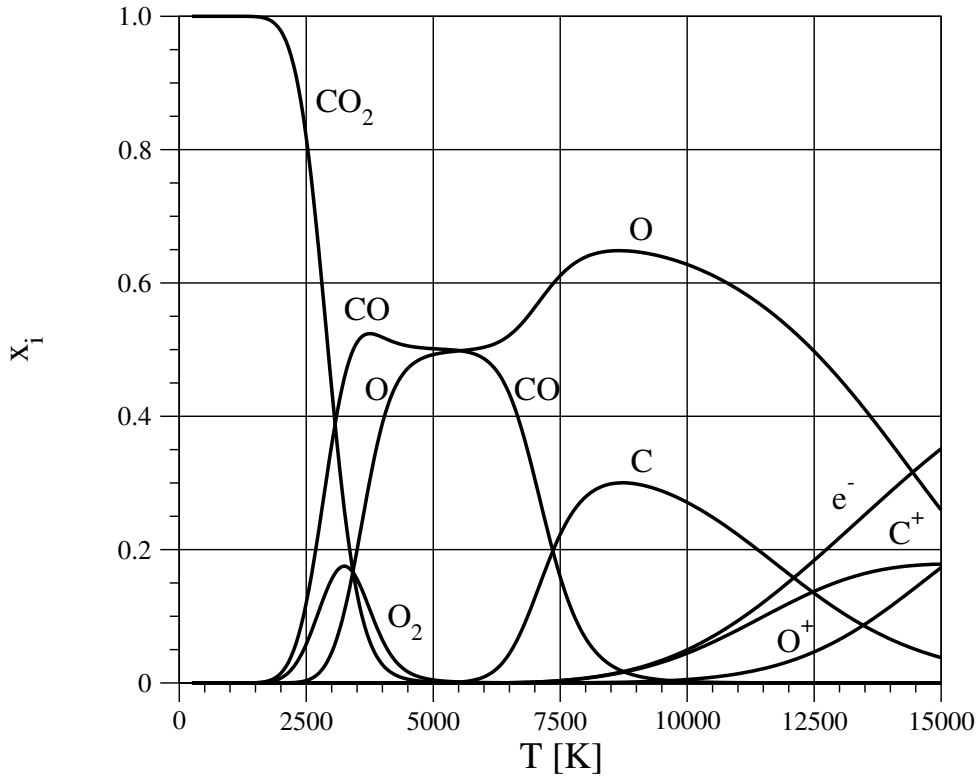

Figure 8: Components of carbon dioxide at 1 atm.

The species appearing on the left hand side are the reactants and the one appearing on the right hand side the products; X_i is a dummy symbol for the species i, ν'_{ir} is the stoichiometric coefficient of reactant i and ν''_{ir} is the stoichiometric coefficient for the product i. An elementary reaction r can proceed in both directions and is always reversible; when there is perfect balance between dissociation and recombination the reaction is in chemical equilibrium.

A typical example is the dissociation recombination of oxygen, which is an important reaction for high temperature air chemistry:

$$O_2 + X \rightleftarrows O + O + X \tag{37}$$

Molecular oxygen O_2 collides with a third body X and dissociates in two oxygen atoms O if the collision energy is enough to activate the reaction. In the reverse reaction two oxygen atoms collide with the third body and recombine into one oxygen molecule if the third body can carry out the energy released in the recombination. It should be noticed that the third body does not change its chemical nature in the reaction.

In accordance with the Law of Mass Action and experimental evidence (Vincenti and Kruger, 1965), the net rate of production of species i by the elementary reaction r just introduced (Eq. 36) is:

$$\dot{w}_{ir} = M_i \left\{ \underbrace{(\nu''_{ir} - \nu'_{ir}) k_{fr} \prod_{j=1}^{N_S} \left(\frac{\rho_j}{M_j} \right)^{\nu'_{jr}}}_{production\ (forward)\ rate} - \underbrace{(\nu''_{ir} - \nu'_{ir}) k_{br} \prod_{j=1}^{N_S} \left(\frac{\rho_j}{M_j} \right)^{\nu''_{jr}}}_{destruction\ (backward)\ rate} \right\} \tag{38}$$

Here we have divided the expression for $\dot{w}_{ir}$ into a production term that goes from left to right (in the reaction 37, for example, this corresponds to the creation of O from O_2) and a destruction term that goes from right to left (in the same reaction this corresponds to the disappearance of O into O_2). The rate of production (or destruction) of a substance is proportional to the product of the concentrations of the reactants raised to the stoichiometric coefficient power, the proportionality constant being the reaction rate.

The number of elementary reactions is arbitrary and, if we have N_r of them involving the species i, the production term for this species is obtained by summing over Eq. 38:

$$\dot{w}_i = M_i \sum_{r=1}^{Nr} (\nu''_{ir} - \nu'_{ir}) \left\{ k_{fr} \prod_{j=1}^{N_S} \left(\frac{\rho_j}{M_j} \right)^{\nu'_{jr}} - k_{br} \prod_{j=1}^{N_S} \left(\frac{\rho_j}{M_j} \right)^{\nu''_{jr}} \right\} \tag{39}$$

k_{fr} is the forward reaction rate for the reaction r and k_{br} the backward reaction rate always for the reaction r. This equation should be valid also at equilibrium and the two reaction rates are linked by: $k_{br} = \frac{k_{fr}}{K_{cr}}$, where K_{cr} is the equilibrium constant for the r^{th} reaction. This choice ensures that, if the flow approaches locally the chemical equilibrium, the chemical composition is correctly computed. K_{cr} is linked with the Gibbs free energy and for a perfect gas it is a function only of temperature. Referring to the elementary reaction r (Eq. 36) K_{cr} reads (Anderson, 1989):

$$\log K_{cr}(T) = -\sum_{i=1}^{N_S} \frac{(\nu''_{ir} - \nu'_{ir}) \hat{g}_i(T)}{\mathcal{R}T} - \log(\mathcal{R}T) \sum_{i=1}^{N_S} (\nu''_{ir} - \nu'_{ir}) \tag{40}$$

$\hat{g}_i$ is the Gibbs free energy per unit mole of species i and is equal to $\hat{h}_i - T\hat{s}_i$, where $\hat{h}_i$ and $\hat{s}_i$ are respectively the enthalpy and entropy of species i per unit mole. The same statistical mechanics methods of section 3.1 are used to compute the Gibbs free energy. Two things should be noticed: the first one is that there are as many equilibrium constants K_{cr} as elementary reactions, the second one is that, since K_{cr} is a function of the thermodynamic properties, its effective value is affected by the models used for the computation of these properties. For example we can expect an effect of anharmonicity corrections.

It is possible to derive the forward reaction coefficient from kinetic theory, assuming a known form for the interaction potential, the elementary dissociation-recombination probabilities and the exact distribution functions. In practice this approach is not possible because too much information is missing and a semiempirical formulation, the so called Arrhenius formulation, is used to compute the forward reaction rate:

$$k_{fr} = A_r T^{\eta_r} e^{\frac{-E_{d,r}}{kT}} \tag{41}$$

$A_r > 0$ is a constant factor, η_r a positive or negative exponent and $E_{d,r}$ is the so-called activation energy for the r^{th} reaction. It has to be noticed that such an expression is rigorously valid only for thermal equilibrium. k_{fr} is usually computed by fitting experimental data. Large differences exist among various authors, with coefficients often differing by one or more orders of magnitude.

4.3 Air nonequilibrium chemistry model

Air at ambient temperature is a mixture of molecular nitrogen (N_2), molecular oxygen (O_2), argon (Ar), carbon dioxide (CO_2) and neon (Ne) (plus some other minor compo-

nents). The first two species are the dominant ones and, for all the applications of interest here, air can be assumed to be made, in volume, of 79% N_2 and 21% O_2. As temperature increases chemical reactions take place and the initial composition is profoundly changed. At a pressure of 1 atmosphere oxygen begins to dissociate in a temperature range between $2000\,K$ and $4000\,K$. The lower the pressure, the lower the temperature at which the dissociation starts and ends. At $100\,Pa$ oxygen is fully dissociated at $3000\,K$ and at $100000\,Pa$ at $5000\,K$. Molecular nitrogen begins to dissociate by reaction with oxygen atoms to produce nitric oxide NO (this happens above $2000\,K$) and then the main phase of dissociation takes place between $3500\,K$ and $8000\,K$. Nitric oxide ion NO^+ starts to appear around $4000\,K$; O^+ and N^+ above $6000\,K$. Therefore, depending on the temperature and pressure range, we can distinguish among three main mixtures models:

- When the degree of ionization is negligible; air is well represented by a five species mixture (air-5): O_2, N_2, NO, O, N.
- When the degree of ionization is not any more negligible, but temperature is sufficiently low; air is well represented by a seven species mixture (air-7): O_2, N_2, NO, O, N, NO^+, e^-.
- When the temperature is higher than in the previous case; air is represented by an eleven species mixture (air-11): O_2, N_2, NO, O, N, O_2^+, N_2^+, NO^+, O^+, N^+, e^-.

A suitable set of chemical reactions is needed to take into account all these phenomena. In air we can have seven main groups of reaction (Park, 1990, 1993; Gupta et al., 1990) that are detailed in Table 1.

- Thermal dissociation of O_2, N_2 and NO molecules by collisions with heavy particles (i.e. all the species except the free electrons); a priori anyone of the heavy particle species is involved (Park, 1993), but in some reaction models (Gupta et al., 1990) only some of them are taken into account. Park (Park, 1990, 1993) considers for the dissociation of N_2 also the electrons as possible third body.
- Bimolecular exchange reactions involving NO: $O_2 + N \rightleftarrows NO + O$ and $N_2 + O \rightleftarrows NO + N$. They are the most important reactions for NO production and the latter removes N_2 from the system even more efficiently than the dissociation reaction.
- Associative ionization and its reverse dissociative neutralization. The first reaction of this group in Table 1 is almost immediately triggered by the presence of N and O atoms.
- Charge exchange reactions. NO^+, N_2^+, O_2^+ are created by associative ionization and are converted into other ions. It is interesting to notice that, if the last group of reactions (impact ionization) is negligible, atomic ion species cannot be generated directly but only through charge exchange reactions.
- Heavy particle impact ionization. These reactions are present only in some reaction schemes (Gupta et al., 1990) and they have very little effect, their activation energy being very high.

Thermal dissociation
$O_2 + X \rightleftarrows O + O + X$ $N_2 + X \rightleftarrows N + N + X$ $NO + X \rightleftarrows N + O + X$
Bimolecular exchange
$O_2 + N \rightleftarrows NO + O$ $N_2 + O \rightleftarrows NO + N$
Associative ionization-dissociative recombination
$N + O \rightleftarrows NO^+ + e^-$ $N + N \rightleftarrows N_2^+ + e^-$ $O + O \rightleftarrows O_2^+ + e^-$
Charge exchange
$NO^+ + O \rightleftarrows N^+ + O_2$ $O_2^+ + N \rightleftarrows N^+ + O_2$ $O^+ + NO \rightleftarrows N^+ + O_2$ $N^+ + N_2 \rightleftarrows N_2^+ + N$ $O_2^+ + N_2 \rightleftarrows N_2^+ + O_2$ $O^+ + N_2 \rightleftarrows N_2^+ + O$ $NO^+ + N \rightleftarrows N_2^+ + O$ $O_2^+ + O \rightleftarrows O^+ + O_2$ $NO^+ + N \rightleftarrows O^+ + N_2$ $NO^+ + O_2 \rightleftarrows O_2^+ + NO$ $NO^+ + O \rightleftarrows O_2^+ + N$
Heavy particle impact ionization
$O_2 + N_2 \rightleftarrows NO + NO^+ + e^-$ $NO + X \rightleftarrows NO^+ + e^- + X$
Electron impact ionization
$O + e^- \rightleftarrows O^+ + e^- + e^-$ $N + e^- \rightleftarrows N^+ + e^- + e^-$

Table 1: Chemical reactions scheme for 11 species air (from Ref. (Gupta et al., 1990; Park, 1993))

- Electron impact ionization of N and O species. They have a very high activation energy, but once they are triggered, they lead to an exponential increase of the free electrons number density.

4.4 Catalycity

In a typical very high speed flight, the gas surrounding an aerospace vehicle is dissociated. In such circumstances, atomic species can recombine not only in the boundary layer, but also at the vehicle surface, thus releasing the reaction energy and increasing the thermal load; therefore his effect should be taken into account when computing the heat flux experienced by a flying vehicle.

A material can have different behaviours with respect to the recombination of atoms impinging its surface. When the material surface is completely inert with respect to atomic recombination we say that it is a noncatalytic wall, when, on the opposite, it promotes the recombination of all the impinging atoms we say that is a fully catalytic wall. The latter definition needs some more observations. We recall that a catalyzer promotes a chemical reaction, but it does not alter its final state. In particular, a catalyzed reaction cannot go beyond the local equilibrium conditions for the reaction itself. The definition of fully catalytic wall as a wall that promotes the recombination of all the atoms impinging the wall itself is, therefore, not correct and it would be better to define as fully catalytic wall a material that, in the limit, allows a local gas composition equal to the equilibrium one. In literature such a wall is often known as local equilibrium wall. When the material is neither noncatalytic nor fully catalytic it is called a partially catalytic wall.

Many different types of elementary reactions are possible on a surface; a generic set, valid on different kinds of materials, is as follows:

1. Atoms in the gas-phase can be adsorbed by a free active surface site or they can leave the surface by thermal desorption. The adsorbed atoms are called adatoms. The adsorption-desorption reaction is written symbolically as:

$$X + (S) \rightleftarrows (X - S)$$

   (S) is a free active surface site.

2. Atoms in the gas-phase can recombine with adatoms to form a molecule that leaves the surface. This mechanism is known as Eley-Rideal (E-R) recombination.

$$Y + (X - S) \rightarrow XY + (S)$$

3. Adatoms migrate on the surface and recombine together in a molecule that leaves the surface. This mechanism is known as Langmuir-Hilsenwood (L-H) recombination.

$$(Y - S) + (X - S) \rightarrow XY + 2(S)$$

4. Molecules in the gas-phase can be adsorbed by a free site and released by thermal desorption. This process usually does not contribute to the heat release, unless the adsorbed molecule is highly excited and releases the excess of energy to the surface, but it can modify the number of free sites and, therefore, the efficiency of E-R and L-H reactions.

5. Molecules are adsorbed on the surface and dissociated (dissociative adsorption): it is in practice the reverse of the E-R and L-H reactions. This reaction can happen for O_2 molecule on metallic surfaces (Reggiani et al., 1996).

The final goal is to determine the rate of production or destruction of each species due to the surface reactions by summing up over all the elementary steps: this gives the heterogeneous wall reaction rate $\dot{w}_{i,cat}$ (mass of species i produced or destroyed per unit area and per unit time).

Next to the surface, the mechanism that feeds the i species from the bulk of the gas to the surface itself is diffusion. Therefore, at steady state, the net amount of species i produced or destroyed by catalytic reactions has to be balanced by the diffusion flux of species i itself.

$$\vec{J}_{i,w} \cdot \vec{n}_w = \dot{w}_{i,cat} \tag{42}$$

(where $\vec{n}_w$ is the normal to the wall, oriented from the gas towards the wall). This expression is also the boundary condition for the species continuity equations (Eq. 3).

For practical applications the wall production rate $\dot{w}_{i,cat}$ is often expressed in a simplified form. The simplest one is to assume that a first order reaction is happening at the wall. In this case, assuming that species i is recombining at the wall, the heterogeneous wall reaction rate reads:

$$\dot{w}_{i,cat} = K_{i,w} \rho_w y_{i,w} \tag{43}$$

$K_{i,w}$ is the catalytic speed for species i (it has dimensions m/s). It is a global index that hides completely every detail of the reactions taking place at the wall.

A more sophisticated approach is to define a suitable recombination probability. Let $\mathcal{M}_i^{\downarrow}$ be the number flux of species i impinging the surface and $\mathcal{M}_{i,rec}$ the number flux of i species recombining at the surface. The recombination probability γ_i is defined as:

$$\gamma_i = \frac{\mathcal{M}_{i,rec}}{\mathcal{M}_i^{\downarrow}} \tag{44}$$

The flux impinging the surface is $\mathcal{M}_i^{\downarrow}$ and the flux leaving the surface is $\mathcal{M}_i^{\downarrow} - M_{i,rec} = (1-\gamma_i)\mathcal{M}_i^{\downarrow}$. The net flux $\vec{J}_{i,w} \cdot \vec{n}_w$ is equal to the difference of the two multiplied by the i species mass and therefore to $\gamma_i m_i \mathcal{M}_i^{\downarrow}$. From the last statement we deduce:

$$\dot{w}_{i,cat} = \gamma_i m_i \mathcal{M}_i^{\downarrow} \tag{45}$$

Kinetic theory provides an expression for the impinging flux $\mathcal{M}_i^{\downarrow}$. Two different results are possible, depending on the expression used for the particles distribution function at the wall. If the Maxwell distribution is used the impinging flux $\mathcal{M}_i^{\downarrow}$ reads:

$$\mathcal{M}_i^{\downarrow} = n_i \sqrt{\frac{kT_w}{2\pi m_i}} \tag{46}$$

If the Chapman-Enskog perturbation term ϕ_i (see Sec. 5.2) is added it reads instead:

$$\mathcal{M}_i^{\downarrow} = n_i \sqrt{\frac{kT_w}{2\pi m_i}} + \frac{1}{2m_i} \vec{J}_i \cdot \vec{n}_w \tag{47}$$

In the first case the wall reaction rate reads (we have used Eq. 42):

$$\dot{w}_{i,cat} = \gamma_i m_i n_i \sqrt{\frac{kT_w}{2\pi m_i}} \tag{48}$$

In the second one:

$$\dot{w}_{i,cat} = \frac{2\gamma_i}{2-\gamma_i} m_i n_i \sqrt{\frac{kT_w}{2\pi m_i}} \tag{49}$$

The last two results are practically identical for $\gamma_i \ll 1$, but when $\gamma_i \to 1$ the difference is appreciable. In effect the right expression is the latter, because the wall reactions perturb the distribution function making it non-Maxwellian and it is the expression that has preferably to be used.

The expressions given in Eqs. 43, 48 and 49 show some inconsistencies. The first is in the link between $K_{i,w}$ and γ_i, that changes depending if we choose Eqs. 43 and 48 or Eqs. 43 and 49. In one case the relation is $K_{i,w} = \gamma_i \sqrt{\frac{kT_w}{2\pi m_i}}$ (known also as Hertz-Knudsen relation) and in the other $K_{i,w} = \frac{2\gamma_i}{2-\gamma_i} \sqrt{\frac{kT_w}{2\pi m_i}}$. The other inconsistency is that none of the above formulations gives a wall chemical composition that tends correctly to the local equilibrium composition limit for a fully catalytic wall, i.e. $K_{i,w} \to \infty$ and $\gamma_i = 1$ respectively. The former condition implies $y_{i,w} = 0$ and the latter $y_{i,w}$ equal to a small, but finite, value that is, in general, different from the local equilibrium one. This inconsistency, however, can be tolerated in our applications because the practically sustainable wall temperatures allow only a negligible equilibrium atomic concentrations.

5 Transport properties

Transport fluxes, i.e. diffusion flux appearing in the species continuity equations (Eq. 7), stress tensor appearing in the momentum equation (Eq. 8) and heat flux appearing in the energy equation (Eq. 11) are computed by the kinetic theory of gases (Chapman and Cowling, 1970; Ferziger and Kaper, 1972; Giovangigli, 1999; Hirschfelder et al., 1964).

The kinetic theory approach we will present in the next sections is rigorously valid under the following assumptions:

$Kn \ll 1$. As already mentioned in Sec. 2, the Knudsen number Kn being small, the gas mixture is collision-dominated and the Navier-Stokes equations are the right governing equations.

No chemical reactions. Ern and Giovangigli (Giovangigli, 1999) have shown that chemical reactions do not influence the transport properties if the characteristic time for chemistry is larger than that for collisions implied in transport phenomena. Therefore, for the sake of transport property computation we assume the gas mixture to be frozen.

No internal energy. The internal energy is not taken into account when deriving transport coefficients. The influence of the internal degrees of freedom on transport properties is addressed in various specialized publications cited in general Refs. (Ferziger and Kaper, 1972; Giovangigli, 1999). Indeed, a rigorous treatment including the internal energy leads to transport collision integrals difficult to estimate with accuracy in high-temperature applications. As a matter of fact, the influence of internal degrees of freedom on properties such as viscosity can be neglected. It is retained instead for diffusion and thermal conductivity by means of a simple correction due to Eucken (Chapman and Cowling, 1970; Hirschfelder et al., 1964; Ferziger and Kaper, 1972).

When the gas mixture under study is ionized we make the additional assumptions:

$\lambda_D \ll L$. The Debye length λ_D being smaller than a reference length L in the flow, quasi-neutrality of the plasma is prescribed.

$\Lambda \gg 1$. The plasma parameter Λ is proportional to the number of electrons in a sphere of radius equal to the Debye length. If the plasma parameter is sufficiently large, charged particle interactions can be treated as binary collisions with Debye-Hückel screening of the Coulomb potential using the usual collision operator of Boltzmann equation (Delcroix and Bers, 1994).

$\varepsilon = \sqrt{m_e/m_h} \ll 1$. Our gas mixture is composed of N_S species. The electron mass reads m_e. A characteristic mass for heavy particles is given by m_h. This hypothesis allows to simplify transport fluxes and transport coefficients evaluations.

$|T_e - T_h| \ll T_e \sim T_h$. Due to the small electron heavy-particle mass-ratio, electron temperature T_e can differ from heavy particle temperature T_h. The case of weak thermal nonequilibrium is studied here. Thermal equilibrium formulation can be recovered by setting: $T_h = T_e = T$.

$\boldsymbol{\beta_e \ll Kn}$. The Hall parameter of electrons β_e is assumed to be smaller than the Knudsen number. Thus, the magnetic field influence on transport properties remains negligible, the plasma is unmagnetized (Magin and Degrez, 2004b). The approach followed here can be generalized to derive transport properties sensitive to a magnetic field.

Finally, to simplify the notation we will indicate with $\mathcal{S}$ the set of all mixture components, including free electrons and with $\mathcal{H}$ the set of heavy particles, i.e. the mixture components minus the free electrons.

5.1 Boltzmann equation

The exact representation of the mixture state is not only impossible because it requires the knowledge of velocity, position and internal state of every particle in the mixture, but is also redundant for our continuum description. It seems therefore more practical and convenient to use a statistical approach that, by its own nature, gives the "global" behaviour of the system under investigation.

Consider a particle belonging to species i (for simplicity we assume it has no internal degrees of freedom): its state is completely characterized by its position $\vec{r}$ and its velocity $\vec{c}_i$. The six-dimensional space having as components the three components of $\vec{r}$ and the three components of $\vec{c}_i$ is called the phase space. In the spirit of the continuum description, it would be enough to have a function $f_i(\vec{r}, \vec{c}_i, t)$ that gives the expected amount of i species particles in an elementary volume $d\vec{r}d\vec{c}_i$ of the phase space. In other words, $N_i = f_i(\vec{r}, \vec{c}_i, t)d\vec{r}d\vec{c}_i$ is the expected number of i species particles in the volume element $d\vec{r}$ located at $\vec{r}$, whose velocities lies in the interval $d\vec{c}_i$ about velocity $\vec{c}_i$ at time t. Integration with respect to $\vec{r}$ and $\vec{c}_i$ gives the total number of i species particles in the system. Integration with respect to $\vec{c}_i$ gives the the total number of i species particles in the volume $d\vec{r}$ and the number density n_i of i species is this number divided by $d\vec{r}$:

$$n_i(\vec{r}, t) = \int f_i(\vec{r}, \vec{c}_i, t)d\vec{c}_i \tag{50}$$

(the integration extends over the full velocity range). The partial density reads $\rho_i = m_i n_i$ where m_i is the mass of the single species particle i.

If $\varphi_i(\vec{r}, \vec{c}_i, t)$ is a generic property for species i, function of the particle velocity, its average value is:

$$\overline{\varphi}_i(\vec{r}, t) = \frac{1}{n_i(\vec{r}, t)} \int \varphi_i(\vec{r}, \vec{c}_i, t) f_i(\vec{r}, \vec{c}_i, t)d\vec{c}_i \tag{51}$$

For example average velocity of species i (the same as the one defined in section 2.1) is:

$$\vec{v}_i(\vec{r}, t) = \frac{1}{n_i(\vec{r}, t)} \int \vec{c}_i f_i(\vec{r}, \vec{c}_i, t)d\vec{c}_i \tag{52}$$

The mixture mass average velocity is identical to the one defined by Eq. 2. The difference between the species velocity of particle i and the mixture average velocity is the peculiar velocity of species i:

$$\vec{C}_i = \vec{c}_i - \vec{v}$$

The peculiar velocity is linked with the thermal motion of the molecules: in a mixture at rest, without macroscopic gradients, particles are still subject to Brownian motion

and this motion is nothing else than the peculiar velocity. The average kinetic energy associated with the peculiar velocity may be identified as the translational component of the internal energy of each mixture component:

$$T_i(\vec{r},t) = \frac{1}{\frac{3}{2}kn_i}\int \frac{1}{2}m_i C_i^2 f_i(\vec{r},\vec{c}_i,t)d\vec{c}_i \tag{53}$$

In our case $T_i = T_e$ for free electrons and $T_i = T_h$ for all the remaining mixture components.

In a gas under nonequilibrium conditions, gradients exist in one or more of the macroscopic physical properties of the system: composition, velocity, temperature. The gradients of these properties result in the molecular transport of mass, momentum and energy through the mixture. The flux vector associated with the transport of the generic property φ_i is:

$$\vec{\Phi}_i(\vec{r},t) = \int \varphi_i(\vec{r},\vec{c}_i,t)\vec{C}_i f_i(\vec{r},\vec{c}_i,t)d\vec{c}_i \tag{54}$$

We point out that the velocity with which φ_i is transported is the peculiar velocity $\vec{C}_i$ of i species particle and not the total velocity $\vec{c}_i = \vec{C}_i + \vec{v}$. In effect we are considering the transport of φ_i through the mixture and the mixture average velocity $\vec{v}$ is responsible for the transport of φ_i with respect to a fixed reference, but not through the mixture, that is the task of the peculiar velocity.

We notice that, once the distribution function is known, we can completely determine the hydrodynamic state of the mixture, i.e. density velocity, energy and their respective fluxes.

Therefore it is time to introduce Boltzmann equation which governs the i species distribution function evolution:

$$\frac{\partial f_i}{\partial t} + \vec{c}_i \cdot \nabla_{\vec{r}} f_i + \frac{\vec{F}_i}{m_i} \cdot \nabla_{\vec{c}_i} f_i = \sum_{j\in\mathcal{S}} J_{ij}(f_i, f_j) \tag{55}$$

Or, in compact notation:

$$\mathcal{D}_i(f_i) = J_i \tag{56}$$

The left hand side is the streaming operator and gives the change of the distribution function due to convection and the effect of the body forces $\vec{F}_i$ on the particles; the right hand side is the collision operator and gives the change in the distribution function due to the collisional processes happening into the flow (Chapman and Cowling, 1970; Ferziger and Kaper, 1972; Hirschfelder et al., 1964).

The total rate of change of the generic $\varphi_i(\vec{r},\vec{c}_i,t)$ property for species i is obtained multiplying the Boltzmann equation (Eq. 55) by φ_i itself and integrating over $\vec{c}_i$: the equation thus obtained is called the *equation of change of the property* φ_i (Chapman and Cowling, 1970; Ferziger and Kaper, 1972; Hirschfelder et al., 1964). Using the compact form of the Boltzmann equation it writes as:

$$\int \varphi_i \mathcal{D}_i(f_i)d\vec{c}_i = \int \varphi_i J_i d\vec{c}_i = n_i \left(\overline{\frac{\partial \varphi_i}{\partial t}}\right)_{coll} \tag{57}$$

The term

$$\left(\overline{\frac{\partial \varphi_i}{\partial t}}\right)_{coll} = \frac{1}{n_i}\sum_{j\in\mathcal{S}}\int \varphi_i(\vec{r},\vec{c}_i,t)J_{ij}(f_i,f_j)d\vec{c}_i$$

is the rate of change of property φ_i due to particle collisions. The equation of change for the mixture property $\varphi = \frac{1}{n}\sum_{i\in\mathcal{S}} n_i\varphi_i$ is obtained by summing up over all the species the equation of change.

The mixture governing equations that have been presented in Sec. 2 can be obtained from the equation of change (Mitchner and Kruger, 1973; Chapman and Cowling, 1970).

Species continuity. Identifying φ_i with the mass m_i of species i, Eq. 57 gives the species continuity equation (i.e. Eq. 7 of Sec. 2.2. We notice that in Eq. 7 the chemical production term is included too).

Mixture momentum. Identifying now φ_i with the species momentum $m_i\vec{c}_i$ and summing over all the species, the mixture momentum equation is recovered (i.e. Eq. 8 of Sec 2.3). The change in momentum due to the collisional operator is zero because of the principle of conservation of momentum during collisions.

Mixture energy. Finally identifying φ_i with the species total energy $\frac{1}{2}m_ic_i^2$ and summing over the species the mixture energy equation is recovered (i.e. Eq. 11 of Sec. 2.4, where also the contribution of species internal energy is taken into account). The change in energy due to the collisional operator is zero too, because of the principle of conservation of energy during collisions.

A comparison among the mixture equations obtained from the equations of change and the ones presented in Sec. 2, allows one to do the following identifications:

Diffusion flux. The diffusion flux (Eq. 5) defined for the species continuity equation (Eq. 7) is given by:

$$\rho_i\vec{V}_i = \int m_i\vec{C}_i f_i(\vec{r},\vec{c}_i,t)d\vec{c}_i \tag{58}$$

Stress tensor. The pressure viscous tensor $-p\bar{\bar{I}}+\bar{\bar{\tau}}$ in the momentum (Eq. 8) and energy (Eq. 11) equations is given by the sum of the species momentum fluxes $\bar{\bar{\mathcal{P}}}_i$:

$$-p\bar{\bar{I}} + \bar{\bar{\tau}} = \sum_{i\in\mathcal{S}}\bar{\bar{\mathcal{P}}}_i = \sum_{i\in\mathcal{S}}\int m_i\vec{C}_i\otimes\vec{C}_i f_i(\vec{r},\vec{c}_i,t)d\vec{c}_i \tag{59}$$

Where $\bar{\bar{I}}$ is the unit tensor.

Heat flux. The heat flux vector $\vec{q}$ in the energy equation (Eq. 11) is given by the sum of the species heat fluxes $\vec{q}_i$:

$$\vec{q} = \sum_{i\in\mathcal{S}}\vec{q}_i = \sum_{i\in\mathcal{S}}\int \frac{1}{2}m_iC_i^2\vec{C}_i f_i(\vec{r},\vec{c}_i,t)d\vec{c}_i \tag{60}$$

As one can remark, the transport fluxes are function, among other things, of the distribution function f_i. If the distribution function, in its turn, *has a one to one correspondence with the macroscopic variables characterizing the mixture*, the governing equations become self-contained, because transport fluxes can be expressed as suitable functions of macroscopic variables.

5.2 Chapman-Enskog method

The Chapman-Enskog method gives the transport fluxes (Eq. 58, 59, 60) as linear functions of the macroscopic variable gradients through proportionality scalar quantities, the transport coefficients. It is important to point out that the method is rigorously valid for small Knudsen number and weak deviation from thermal equilibrium. We distinguish between heavy particles, index h, and free electrons, index e. We allow heavy particles temperature T_h and electrons temperature T_e to differ. The case of equal temperatures is simply recovered by taking: $T_h = T_e = T$.

The distribution function is developed in a series expansion with respect to a small perturbation parameter ϵ proportional to the Knudsen number (Chapman and Cowling, 1970; Ferziger and Kaper, 1972; Hirschfelder et al., 1964). Stopping the expansion to the first two terms of the series one has for species i:

$$f_i^{CE} = f_i^{(0)} + \epsilon f_i^{(1)} = f_i^{(0)}(1 + \epsilon\phi_i) \tag{61}$$

The approximate solution of the Boltzmann equation is obtained by inserting the series expansion into Eq. 55 and equating the coefficients of equal powers of ϵ [for more details see (Chapman and Cowling, 1970; Ferziger and Kaper, 1972; Hirschfelder et al., 1964)]. The expression for the zero order approximation f_i^0 is:

$$f_i^{(0)} = n_i \left(\frac{m_i}{2\pi k T_i}\right)^{\frac{3}{2}} e^{-\frac{m_i C_i^2}{2kT_i}} \tag{62}$$

(We recall that in our case $T_i = T_e$ for free electrons and $T_i = T_h$ for all the remaining mixture components). This expression is the Maxwell distribution function and is assumed by the gas particles in case of thermal equilibrium. The equations we obtain sticking the Maxwell distribution into the equation of change Eq. 57 are the Euler equations. They are characterized by the absence of dissipation and therefore of transport fluxes, i.e. diffusion flux and heat flux are identically zero and the stress tensor reduces to the thermodynamic pressure p.

The perturbation term ϕ_i is solution of the following linear integral equation:

$$\begin{aligned} n^2 I_i(\phi) = -f_i^0 \Bigg[& \frac{n}{n_i}\Theta_i \vec{C}_i \cdot \vec{d}_i + \left(\vec{\mathscr{C}}_i^{\,2} - \frac{5}{2}\right)\vec{C}_i \cdot \nabla \log T_i \\ & + 2(1-\delta_{ie})\left(\vec{\mathscr{C}}_i \otimes \vec{\mathscr{C}}_i - \frac{\vec{\mathscr{C}}_i^{\,2}}{3}\bar{\bar{I}}\right) : \nabla\vec{v} \Bigg] \end{aligned} \tag{63}$$

The term $I_i(\phi)$ is a linearized collisional operator defined in (Magin and Degrez, 2004b). The thermal nonequilibrium parameter Θ is defined as: $\Theta_i = T_h/T_i$. $\vec{\mathscr{C}}_i$ is a non-dimensional velocity that writes:

$$\vec{\mathscr{C}}_i = \left(\frac{m_i}{2kT_i}\right)^{\frac{1}{2}} \vec{C}_i$$

The most general form of the unknown function ϕ_i is:

$$\phi_i = -\frac{1}{n}\left[\vec{A}_i^h \cdot \nabla \log(T_h) + \vec{A}_i^e \cdot \nabla \log(T_e) + \bar{\bar{B}}_i : \nabla\vec{v} + \sum_{j\in\mathcal{S}} \vec{D}_i^j \cdot \vec{d}_j\right] \tag{64}$$

$\vec{d_i}$ is a vector of driving forces that reads:

$$\vec{d_i} = \frac{\nabla p_i}{nkT_h} - \frac{y_i p \nabla \log p}{nkT_h} + (y_i q - x_i q_i)\frac{\vec{E}}{kT_h} \tag{65}$$

where $\vec{E}$ is the electric field acting on charged particles. The driving forces are not linearly independent:

$$\sum_{i \in \mathcal{S}} \vec{d_i} = 0 \tag{66}$$

If the approximate solution $f_i^{CE} = f_i^0(1 + \epsilon\phi_i)$ is inserted into the equation of change Eq. 57, the Navier-Stokes equations are obtained. The diffusion flux, the pressure viscous tensor and the heat flux are obtained by computing the transport fluxes (Eqs. 58, 59, 60) with the approximate value of the distribution function.

The unknown coefficients $\vec{A}_i^h$, $\vec{A}_i^e$, $\bar{\bar{B}}_i$ and $\vec{D}_i^j$ entering the expression 64 for ϕ_i are functions only of the peculiar velocities of mixture components and must take the form:

$$\vec{A}_i^h = A_i^h(C_i)\,\vec{C}_i \tag{67a}$$
$$\vec{A}_i^e = A_i^e(C_i)\,\vec{C}_i \tag{67b}$$
$$\bar{\bar{B}}_i = B_i(C_i)\left(\vec{C}_i \otimes \vec{C}_i - \frac{C_i^2}{3}\bar{\bar{I}}\right) \tag{67c}$$
$$\vec{D}_i^j = D_i^j(C_i)\,\vec{C}_i \tag{67d}$$

They are solution of the integral equations:

$$I_i\left(\vec{D}^{\,j}\right) = \frac{1}{n_i} f_i^0(\delta_{ij} - y_i)\,\Theta_i \vec{C}_i \tag{68a}$$
$$I_i\left(\vec{A}^{\,h}\right) = \frac{1}{n} f_i^0(1 - \delta_{ie})\left(\vec{\mathscr{C}}_i^{\,2} - \frac{5}{2}\right)\vec{C}_i \tag{68b}$$
$$I_i\left(\vec{A}^{\,e}\right) = \frac{1}{n} f_i^0 \delta_{ie}\left(\vec{\mathscr{C}}_i^{\,2} - \frac{5}{2}\right)\vec{C}_i \tag{68c}$$
$$I_i\left(\bar{\bar{B}}\right) = \frac{2}{n} f_i^0(1 - \delta_{ie})\left(\vec{\mathscr{C}}_i \otimes \vec{\mathscr{C}}_i - \frac{\vec{\mathscr{C}}_i^{\,2}}{3}\bar{\bar{I}}\right) \tag{68d}$$

The vectors $\vec{D}^j$ are not linearly independent and the constraint $\sum_j y_j \vec{D}^j = 0$ is imposed in order to derive for diffusion fluxes symmetric expressions in agreement with Onsager's reciprocity relations (Ferziger and Kaper, 1972).

A closed form expression for D_i^j, A_i^h, A_i^e and B_i, solution of the respective integral equations, does not exist: an approximate solution is sought in the form of a finite polynomial expansion. The Sonine polynomials, which have some useful orthogonality properties, are

used (Chapman and Cowling, 1970; Ferziger and Kaper, 1972).

$$\vec{A}_i^h = -\sqrt{\frac{m_i}{2k_BT_i}} \sum_{p\in\mathcal{P}} a_{i,p}^h(\xi)\, S_{\frac{3}{2}}^{(p)}\left(\mathscr{C}_i^{\,2}\right)\vec{\mathscr{C}}_i \tag{69a}$$

$$\vec{A}_i^e = -\sqrt{\frac{m_i}{2k_BT_i}} \sum_{p\in\mathcal{P}} a_{i,p}^e(\xi)\, S_{\frac{3}{2}}^{(p)}\left(\mathscr{C}_i^{\,2}\right)\vec{\mathscr{C}}_i \tag{69b}$$

$$\bar{\bar{B}}_i = \sum_{p\in\mathcal{P}} b_{i,p}(\xi)\, S_{\frac{5}{2}}^{(p)}\left(\mathscr{C}_i^{\,2}\right)\left(\vec{\mathscr{C}}_i\otimes\vec{\mathscr{C}}_i - \frac{\mathscr{C}_i^{\,2}}{3}\bar{\bar{I}}\right) \tag{69c}$$

$$\vec{D}_i^j = \sqrt{\frac{m_i}{2k_BT_i}} \sum_{p\in\mathcal{P}} d_{i,p}^j(\xi)\, S_{\frac{3}{2}}^{(p)}\left(\mathscr{C}_i^{\,2}\right)\vec{\mathscr{C}}_i \tag{69d}$$

where $\mathcal{P} = \{0,\ldots,\xi-1\}$. The accuracy ξ of the approximation depends on how many terms are kept in the polynomial expansion. The sequence is monotonically increasing and converges to the exact solution of the integro-differential equation and so the transport properties computed with the Sonine expansion tend asymptotically to the properties computed with the exact Chapman-Enskog procedure (Ferziger and Kaper, 1972). In the remaining, when talking about the order of approximation in transport properties evaluation, we will mean how many terms are retained in the Sonine polynomial expansion. Substituting Eq. 69d into the integral equation (68a), Eq. 69a into the integral equation (68b), and Eq. 69b into the integral equation (68c), multiplying by the vector $S_{3/2}^{(p)}\left(\mathscr{C}_i^{\,2}\right)\vec{\mathscr{C}}_i$, and integrating over $\vec{c}_i$, the transport systems for diffusion and heat transfer coefficients are obtained. Similarly, substituting Eq. 69c into the integral equation 68d, multiplying by the tensor $S_{5/2}^{(p)}\left(\mathscr{C}_i^{\,2}\right)\left(\vec{\mathscr{C}}_i\otimes\vec{\mathscr{C}}_i - \mathscr{C}_i^{\,2}\,\bar{\bar{I}}/3\right)$ and integrating over $\vec{c}_i$, the transport system for stress tensor coefficients is obtained.

Here we will not go into the details of such a process; we refer to Refs. (Hirschfelder et al., 1964; Chapman and Cowling, 1970; Ferziger and Kaper, 1972; Magin and Degrez, 2004b). In the next sections instead we will give the final expressions for diffusion flux, stress tensor and heat flux along with the linear systems one need to solve in order to compute the associated transport coefficients.

5.3 Diffusion flux

The diffusion flux is obtained by sticking $f_i = f_i^{CE}$ into Eq. 58; the contribution of the Maxwellian part of the distribution function, f_i^0, is zero and also the contribution of the coefficient $\bar{\bar{B}}_i$ of ϕ_i. The final expression is:

$$\rho_i\vec{V}_i = -\rho_i\left(\sum_{j\in\mathcal{S}} D_{ij}\vec{d}_j + D_{Ti}^h\nabla\log T_h + D_{Ti}^e\nabla\log T_e\right) \tag{70}$$

D_{ij} are the multicomponent diffusion coefficients, they are symmetric, $D_{ij} = D_{ji}$ and $D_{ii} > 0$ and the matrix formed by the coefficients is singular. D_{Ti}^h and D_{Ti}^e are the thermal diffusion coefficients. We point out that D_{ij}, D_{Ti}^h and D_{Ti}^e are not linearly independent:

$$\sum_{i\in\mathcal{S}} y_i D_{ij} = 0, \qquad \sum_{i\in\mathcal{S}} y_i D_{Ti}^h = 0, \qquad \sum_{i\in\mathcal{S}} y_i D_{Ti}^e = 0$$

Instead of the thermal diffusion coefficients we can use the thermal diffusion ratios:

$$\sum_{j\in\mathcal{S}} D_{ij}k^h_{Tj} = D^h_{Ti} \tag{71a}$$

$$\sum_{j\in\mathcal{S}} D_{ij}k^e_{Tj} = D^e_{Ti} \tag{71b}$$

$$\sum_{j\in\mathcal{H}} k^h_{Tj} + \frac{T_e}{T_h}k^h_{Te} = 0 \tag{71c}$$

$$\sum_{j\in\mathcal{H}} k^e_{Tj} + \frac{T_e}{T_h}k^e_{Te} = 0 \tag{71d}$$

Constraints 71c and 71d are introduced because the matrix of multicomponent diffusion coefficients is singular. The diffusion flux now reads:

$$\rho_i\vec{V}_i = -\rho_i\sum_{j\in\mathcal{S}}\left(D_{ij}\vec{d}_j + k^h_{Tj}\nabla\log T_h + k^e_{Tj}\nabla\log T_e\right) \tag{72}$$

The multicomponent diffusion coefficients D_{ij} are computed by means of the solution of suitable linear systems. If the Sonine expansion is of order ξ one needs to solve N_S systems each one of dimensions ξN_S by ξN_S. The effective number of operations can be reduced by taking into account the symmetry property of the D_{ij}'s, but it is still a considerable computational load. The thermal diffusion coefficients are computed from the solution of a linear system of dimensions $(\xi+1)N_S$ by $(\xi+1)N_S$.

Due to the high computational cost associated with the evaluation of the multicomponent and thermal diffusion coefficients, it is customary in literature to resort to some kind of Fick's law approximation. The diffusion flux is replaced by an expression of the kind:

$$\rho_i\vec{V}_i = -\rho D^m_i\nabla x_i$$

where D^m_i is a suitable multicomponent binary diffusion coefficient. This approximation does not satisfy the constraint of mass conservation, i.e. Eq. 6, unless all the D^m_i coefficients are equal, and can give very false values for heat flux (Sutton and Gnoffo, 1998). They were probably justified in the early days when computational power was very weak, but not nowadays and they have to be discarded. A more sophisticated approach is due to Ramshaw (Ramshaw, 1990) and is equivalent to the Fick's law plus a correction term to satisfy the mass conservation property. This approach is quite accurate for heat flux determination, but still not satisfactory from the point of view of a strict adherence to kinetic theory.

Stefan-Maxwell equations

In this lecture we propose to use the exact kinetic theory approach to compute the diffusion fluxes, but instead of using Eq. 72 we reverse it; i.e. we express the diffusion driving forces in function of the diffusion velocities. The new equations we obtain are the Stefan-Maxwell equations and they read:

$$\sum_{j\in\mathcal{H}} \hat{G}^{\vec{V}}_{ij}\vec{V}_j = -\vec{d}_i + \frac{\kappa_i}{\kappa_e}\vec{d}_e, \quad i\in\mathcal{H} \tag{73}$$

The Stefan-Maxwell equations keep the same structure independently of the Sonine approximation order. The expression for the coefficients $\hat{G}_{ij}^{\vec{V}}$ is given in Appendix A. The modified driving forces and the electric field coefficients are:

$$\vec{d}_i = \frac{\nabla p_i}{nkT_h} - \frac{y_i p}{nk_B T_h}\nabla \log p + k_{Ti}^h(\xi)\nabla \log T_h + k_{Ti}^e(\xi)\frac{T_i}{T_e}\nabla \log T_e \quad (74a)$$

$$\kappa_i = \frac{1}{k_B T_h}(x_i q_i - y_i q) \quad (74b)$$

The modified driving forces and electric field coefficients are not linearly independent: $\sum_{j\in\mathcal{S}} \vec{d}_j = 0$, $\sum_{j\in\mathcal{S}} \kappa_j = 0$. It is important to point out that the Stefan-Maxwell equations are not linearly independent and have to be supplied with the mass conservation constraint (see Eq. 6): $\sum_{i\in\mathcal{H}} y_i \vec{V}_i = 0$. The electron diffusion velocity is deduced from the ambipolar constraint: $\vec{V}_e = -\sum_{j\in\mathcal{H}} x_j q_j \vec{V}_j/(x_e q_e)$. The ambipolar electric field is given by $\vec{E} = \vec{d}_e/\kappa_e$.

5.4 Heat flux

Due to the small electron heavy particles mass-ratio, the contributions of heavy particles and free electrons to the heat flux vector can be split in two separate parts. This is a fortunate circumstance because in order to compute accurate heat flux values a higher number of terms in the Sonine expansion should be taken for electron contribution compared to heavy particle one (Devoto, 1966, 1967).

5.4.1 Heavy particle heat flux

The heavy particles heat flux reads:

$$\vec{q}_h = -\lambda_h \nabla T_h + \sum_{i\in\mathcal{H}} h_i \rho_i \vec{V}_i + nkT_h \sum_{i\in\mathcal{H}} k_{Ti}^h \vec{V}_i \quad (75)$$

The translational heavy particles thermal conductivity is given, in the second Sonine approximation denoted by $\lambda(2)$, by the solution of the system:

$$\sum_{j\in\mathcal{H}} G_{ij}^{\lambda_h} \alpha_j^{\lambda_h} = x_i, \quad i \in \mathcal{H} \quad (76a)$$

$$\lambda_h(2) = \sum_{j\in\mathcal{H}} \alpha_j^{\lambda_h} x_j \quad (76b)$$

Heavy particle thermal diffusion ratios are then obtained as follows:

$$k_{Ti}^h(2) = \frac{5}{2}\sum_{j\in\mathcal{H}} \Lambda_{ij}^{01} \alpha_j^{\lambda_h}, \quad i \in \mathcal{H} \quad (77)$$

where $\sum_{j\in\mathcal{H}} k_{Tj}^h = 0$ and $k_{Te}^h = 0$. It is important to notice that the translational thermal conductivity and thermal diffusion ratios of heavy particles do not depend on electrons. The expressions of the coefficients $G_{ij}^{\lambda_h}$ and Λ_{ij}^{01} are given in the Appendix A. The term $\sum_{i\in\mathcal{H}} h_i \rho_i \vec{V}_i$ accounts for the heat flux due to the transfer of particles enthalpy, h_i, by means of diffusion.

5.4.2 Electron heat flux

The electrons heat flux reads:

$$\vec{q_e} = -\lambda_e \nabla T_e + h_e \rho_e \vec{V_e} + nkT_h \sum_{i \in \mathcal{H}} k^e_{Ti} \vec{V_i} \tag{78}$$

The electron thermal conductivity reads in the second and third Sonine approximations:

$$\lambda_e(2) = \frac{x_e^2}{\Lambda^{11}_{ee}} \tag{79a}$$

$$\lambda_e(3) = \frac{x_e^2 \Lambda^{22}_{ee}}{\Lambda^{11}_{ee}\Lambda^{22}_{ee} - \left(\Lambda^{12}_{ee}\right)^2} \tag{79b}$$

Electron thermal diffusion ratios k^e_{Ti} are obtained from:

$$k^e_{Ti}\,(2) = \frac{5}{2}\frac{T_e}{T_h} x_e \frac{\Lambda^{01}_{ie}}{\Lambda^{11}_{ee}} \tag{80a}$$

$$k^e_{Ti}\,(3) = \frac{5}{2}\frac{T_e}{T_h} x_e \frac{\Lambda^{01}_{ie}\Lambda^{22}_{ee} - \Lambda^{02}_{ie}\Lambda^{12}_{ee}}{\Lambda^{11}_{ee}\Lambda^{22}_{ee} - \left(\Lambda^{12}_{ee}\right)^2} \tag{80b}$$

where $\sum_{j \in \mathcal{H}} k^e_{Tj} + k^e_{Te} T_e/T_h = 0$. Expressions for the various coefficients are given in Appendix A.

5.4.3 Eucken correction

As already mentioned in Sec. 5, the particles internal energy has not been taken into account in the derivation of the different transport fluxes. Nevertheless it is an experimental evidence that internal energy (Ferziger and Kaper, 1972) affects the heat flux.

The first obvious effect is that internal energy has to be included in the transfer of particles enthalpy by means of diffusion; the second is that internal energy modes change the value of thermal conductivity (Hirschfelder et al., 1964; Ferziger and Kaper, 1972). In the heavy particles heat flux (Eq. 75) one needs to add to the translational thermal conductivity λ_h the "internal" thermal conductivity that can be split into contributions due to rotational (λ_R), vibrational (λ_V) and electronic (λ_E) internal energy modes. It is clear that rotational and vibrational contributions have to be taken into account only for molecules (symbol $\mathcal{H}_p$ being the molecules set). Using the Eucken correction these new contributions read:

$$\lambda_R = \sum_{i \in \mathcal{H}_p} \frac{\rho_i c_{R,i}}{\sum_{j \in \mathcal{H}} x_j / \mathscr{D}_{ij}} \tag{81a}$$

$$\lambda_V = \sum_{i \in \mathcal{H}_p} \frac{\rho_i c_{V,i}}{\sum_{j \in \mathcal{H}} x_j / \mathscr{D}_{ij}} \tag{81b}$$

$$\lambda_E = \sum_{i \in \mathcal{H}} \frac{\rho_i c_{E,i}}{\sum_{j \in \mathcal{H}} x_j / \mathscr{D}_{ij}} \tag{81c}$$

where $c_{R,i}$, $c_{V,i}$, and $c_{E,i}$ are the rotational, vibrational, and electronic species specific heats per unit mass. The coefficients $\mathscr{D}_{ij}$ are the so called binary diffusion coefficients whose expression is given in Appendix A.

The final expression for heavy particles thermal conductivity becomes:

$$\vec{q}_h = -(\lambda_h + \lambda_R + \lambda_V + \lambda_E)\nabla T_h + \sum_{i\in\mathcal{H}} h_i \rho_i \vec{V}_i + nkT_h \sum_{i\in\mathcal{H}} k_{Ti}^h \vec{V}_i \tag{82}$$

5.4.4 LTE heat flux

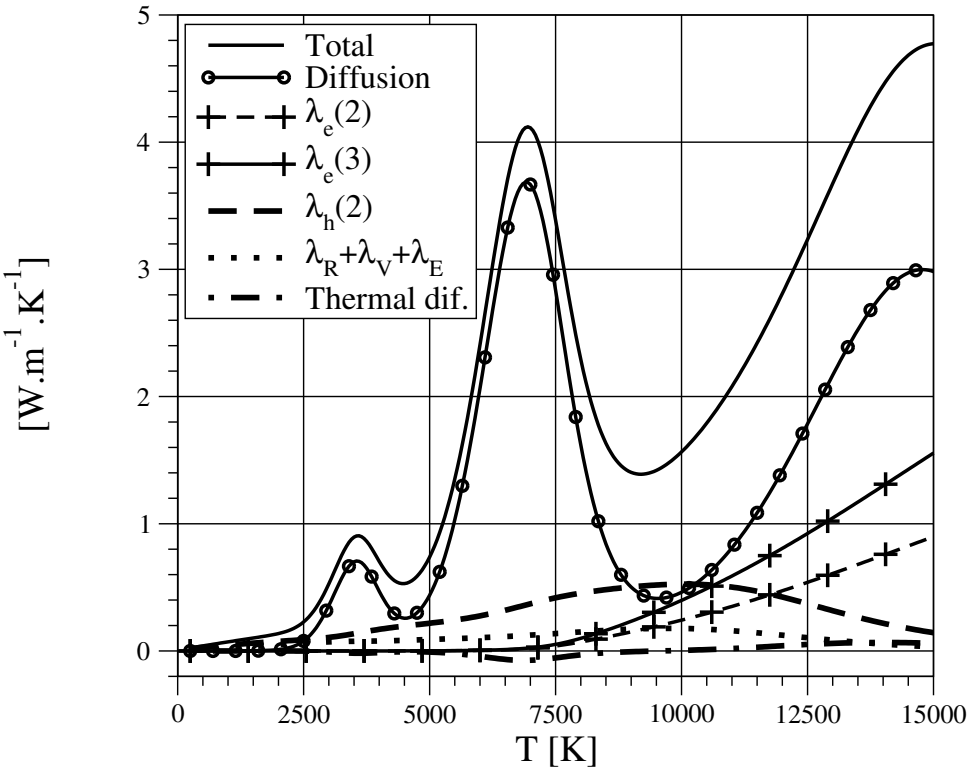

Figure 9: Heat flux components of air, per temperature gradient.

The heat flux components per temperature gradient are compared in Figs. 9 and 10. The diffusion heat flux $\sum_{j\in\mathcal{S}} \rho_j h_j \vec{V}_j$ yields the dominant contribution for temperature ranges 2500-9000 and 11 000-15 000 K for air, and 2000-4500 and 6000-15 000 K for carbon dioxide. The peaks correspond to the dissociation peaks (O_2 and N_2 for air, CO_2 and CO for carbon dioxide), and ionization peaks of atoms (N and O for air, C and O for carbon dioxide). Diffusion velocities are deduced from Eq. 73 in the second Laguerre-Sonine approximation. An electric field, gradients of pressure, temperature, and concentration generate mass fluxes. We envisage the effect of a thermal gradient on the diffusion velocities, in relation with variations of the equilibrium composition and ambipolar electric field. The influence of an external electric field or pressure gradient is not considered. Therefore, the driving forces read $\mathbf{d}_i = (\partial x_i/\partial T)\nabla T - \kappa_i \mathbf{E}$, where $\mathbf{E}$ is the ambipolar field. The electron thermal conductivity λ_e given in Eq. 79 becomes significant beyond 7000 K. The second Laguerre-Sonine approximation underestimates the magnitude of λ_e, the third order approximation is required. The heavy particle thermal conductivity $\lambda_h(2)$ and internal thermal conductivity $\lambda_R + \lambda_V + \lambda_E$ are computed using Eqs. 76 and 81. Their influence is major below 2000 K and between the peaks of diffusion

heat flux. The thermal diffusion heat flux $p \sum_{j \in \mathcal{S}} [k^h_{Tj}(2) + k^e_{Tj}(3)]\ \mathbf{V}_j$ weakly contributes to the total heat flux in LTE plasmas.

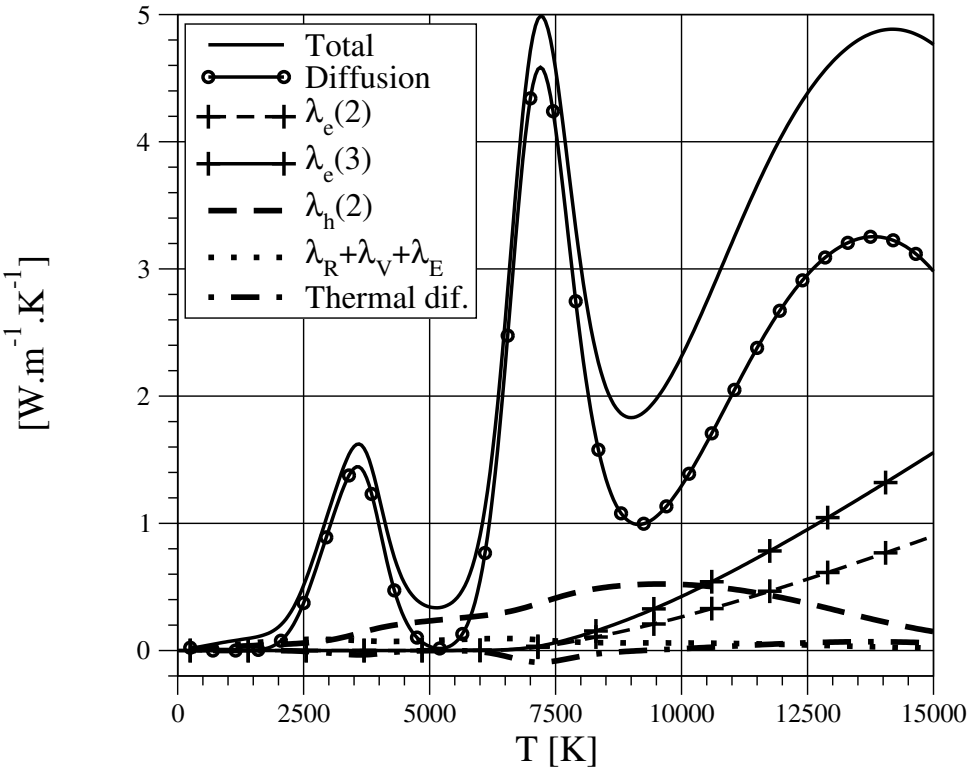

Figure 10: Heat flux components of carbon dioxide, per temperature gradient.

5.5 Stress tensor

The stress tensor expression is:

$$\bar{\bar{\tau}} = \mu \left[\nabla \vec{v} + (\nabla \vec{v})^T \right] - \frac{2}{3} \mu \nabla \cdot \vec{v} \bar{\bar{I}} \tag{83}$$

The shear viscosity coefficient μ is computed, in the first Sonine approximation,as solution of the system:

$$\sum_{j \in \mathcal{H}} G^{\mu}_{ij} \alpha^{\mu}_j = x_i, \quad i \in \mathcal{H} \tag{84a}$$

$$\mu(1) = \sum_{j \in \mathcal{H}} \alpha^{\mu}_j x_j \tag{84b}$$

We notice that the shear viscosity does not depend on electrons. The expression of the coefficients G^{μ}_{ij} is given in Appendix A.

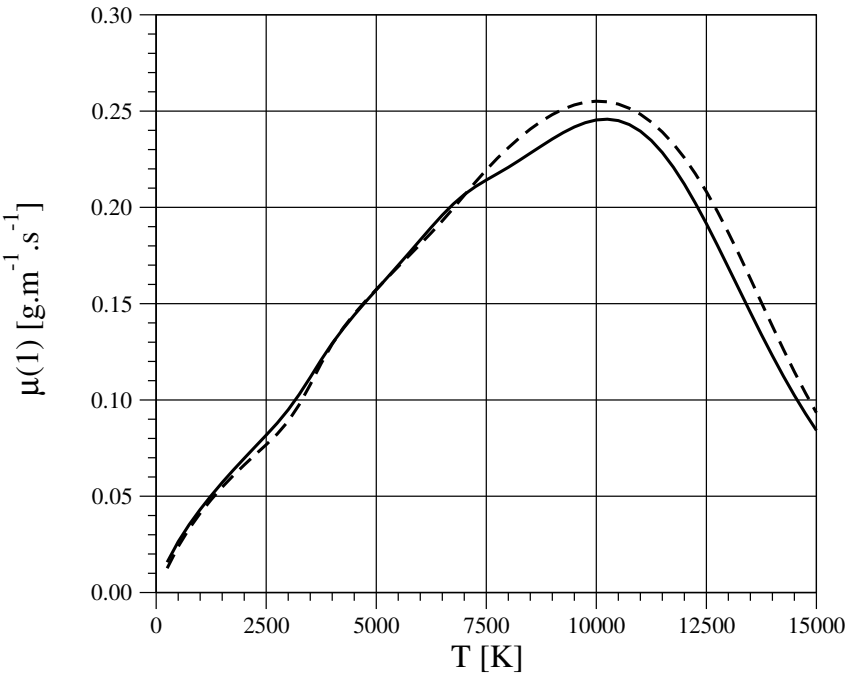

Figure 11: Shear viscosity at 1 *atm*: — air, −− carbon dioxide.

If gas particles have internal energy a new coefficient appears in Eq. 83, the volume viscosity η which multiplies the divergence of velocity term. Volume viscosity is linked with the time-lag necessary to equilibrate internal and translational energies of molecules and results in three additional normal stress components. In multicomponent flow modeling it is usually neglected: the main reason being that the necessary data to correctly computing it are lacking. Experimental results on acoustic waves absorption show that μ and η are of the same order, at least at ambient temperature. Neglecting η has thus no justification a priori. What eventually can be neglected is the influence of the term $\eta\nabla\cdot\vec{v}\bar{\bar{I}}$ on the flow structure. For low Mach number (without strong thermal expansion) flows this can be a good assumption, but for high speed compressible flows it is questionable.

6 CFD example: OREX case

In this section we will show an example of computation of a hypersonic flow field. The main point is to demonstrate the effect of wall catalycity and diffusion fluxes modeling on the heat flux experienced by the flying vehicle. The physico-chemical models used are the ones described in the previous sections.

The Orbital Reentry Experiment (OREX) vehicle is a 50^o spherically blunted cone with a nose radius of $1.35\,m$ and an overall base diameter of $3.4\,m$; the geometry is shown in detail in Fig. 12. The nose cap is made of a monocoque Carbon-Carbon (C/C) material coated with Silicon-Carbide (SiC).

We compare here the computed heat flux in the stagnation region with the one inferred from the temperature measurement of the nose cap back surface. The wall temperature is not uniform on the OREX vehicle heat shield and its distribution is shown in Fig. 13 (Gupta et al., 1996). The peak temperature value is located at the stagnation point and it is equal to $1458\,K$. The computations have been performed for an altitude of $56.9\,km$, which corresponds approximately to the peak heating situation. The freestream conditions are: $p_\infty = 23.7\,Pa$, $T_\infty = 248\,K$, $M_\infty = 17.55$. The axisymmetric computational grid has 65 by 90 cells and it is suitably refined next to the wall and in the shock region to improve both accuracy and stability of the computations. The von Karman Institute code Cosmic (Barbante, 2001) has been used for the computation. Computations have been performed with two different air nonequilibrium chemistry models, air-5 and air-7 (see Sec. 4.3) and the reaction rates set of Gupta (Gupta et al., 1990). Computed heat fluxes are practically identical for the two mixtures.

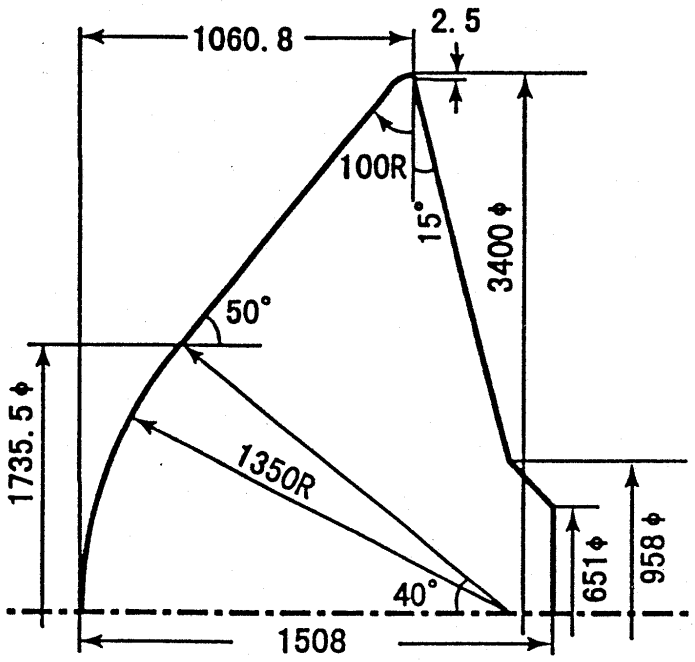

Figure 12: OREX vehicle geometry (from Ref. (Kurotaki, 2000), lengths in mm.)

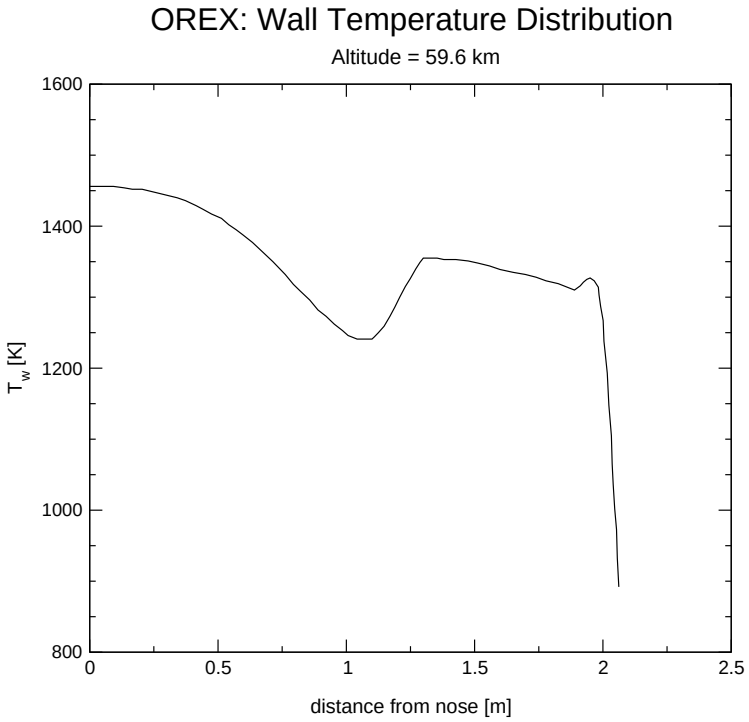

Figure 13: OREX vehicle wall temperature distribution

In Fig. 14 the heat flux on the forebody, computed for different values of the wall catalycity, is shown. The wall heterogeneous catalytic reactions are assumed to be $N + N \rightarrow N_2$ and $O + O \rightarrow O_2$. The recombination probability γ_i (see Eq. 44) is assumed to be equal for both wall reactions. Shown are also the heat flux inferred flight value in the stagnation point and the heat flux distribution computed by Yamamoto (as reported in Ref. (Gupta et al., 1996)) for a noncatalytic wall. The stagnation point heat flux range is between 29 $\frac{W}{cm^2}$ for a noncatalytic wall and 61 $\frac{W}{cm^2}$ for a fully catalytic wall. The heat flux inferred flight value is equal to 39 $\frac{W}{cm^2}$, the Yamamoto computation to 33 $\frac{W}{cm^2}$. We observe that our heat flux distribution for a noncatalytic wall and the Yamamoto's one have the same qualitative behaviour. The Gupta's computation of Ref. (Gupta et al., 1996) (not shown here) has a stagnation point heat flux value of 26 $\frac{W}{cm^2}$ (for noncatalytic wall). We would like to point out the dramatic increase of the heat flux load due to wall catalycity effects: it doubles going from a noncatalytic wall to a fully catalytic one. It is also interesting to note that, even for a low catalytic material as the one used on the nose cap ($\gamma_i \approx 3\,10^{-3}$), the catalytic activity in enough to raise the heat flux by more than 30%. This means that for hypersonic vehicles it is important to develop materials with as low catalycity as possible.

The Stefan-Maxwell equations (Eq. 73) are used to model the diffusion fluxes; by derivation they are equivalent to the exact (in the Chapman-Enskog approximation) diffusion equations (Eq. 70). In literature it is customary instead to use some kind of Fick's law approximation: we would like to briefly point out the effect of different diffusion formulations on the computed heat flux.

The Fick's law approximation (Sutton and Gnoffo, 1998) can be expressed in two different ways; one where the driving force is the mass fraction gradient (hereafter called

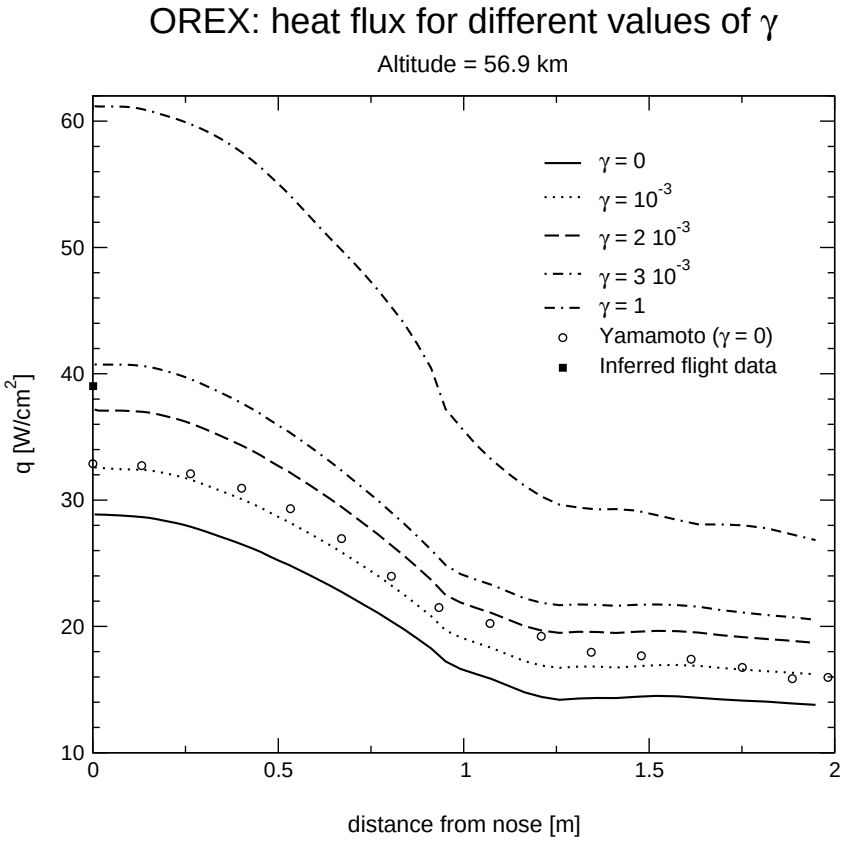

Figure 14: OREX vehicle heat flux for different values of wall catalycity

mass fraction Fick's law) and one where the driving force is the mole fraction gradient (hereafter called mole fraction Fick's law). They read respectively:

$$\vec{J_i} = -\rho D_{im} \nabla y_i \tag{85}$$

where $D_{im} = (1 - x_i) / \sum_{j=1, j \neq i}^{Ns} \frac{x_j}{\mathcal{D}_{ij}}$; and

$$\vec{J_i} = -\rho \frac{M_i}{M} \bar{D}_{im} \nabla x_i \tag{86}$$

where $\bar{D}_{im} = (1 - y_i) / \sum_{j=1, j \neq i}^{Ns} \frac{x_j}{\mathcal{D}_{ij}}$. Such a formulation, although exact for a binary mixture, is incorrect for a multicomponent one ($N_S \geq 3$) because the mass conservation constraint, i.e. $\sum_{i=1}^{N_S} \vec{J_i} = 0$, is not satisfied unless all the coefficients D_{im} or $\bar{D}_{im}$ are equal, which is not true in general.

To overcome such a discrepancy Ramshaw (Ramshaw, 1990) has proposed a different formulation that reads:

$$\vec{J_i} = -\rho \frac{M_i}{M} D_{im} \nabla x_i + y_i \sum_{j=1}^{Ns} \rho \frac{M_j}{M} D_{jm} \nabla x_j \tag{87}$$

In practice it is equivalent to a Fick's law formulation plus a correction term that is added to satisfy the mass conservation constraint.

In order to assess the effect of diffusion modeling on the computed solution, we calculate the OREX case with a recombination probability γ_i equal to 10^{-3} using the two Fick's law formulations and the Ramshaw one in addition to the Stefan-Maxwell.

In Fig. 15 the computed heat flux is shown for the OREX case. The lowest heat flux value is given by mole fraction Fick's law (Eq. 86), the highest by mass fraction Fick's law (Eq. 85). The difference with respect to the Stefan-Maxwell value is (in the stagnation point) of 5.8 % for the former and of 2 % for the latter. The Ramshaw formulation predicts a stagnation point heat flux that is 3.4 % lower than the Stefan-Maxwell one.

The trends predicted here agree with the ones of Ref. (Sutton and Gnoffo, 1998), where it is shown that, for higher freestream Mach number or for higher catalytic activity materials, the difference in computed heat flux can grow up to $40 - 50$ %.

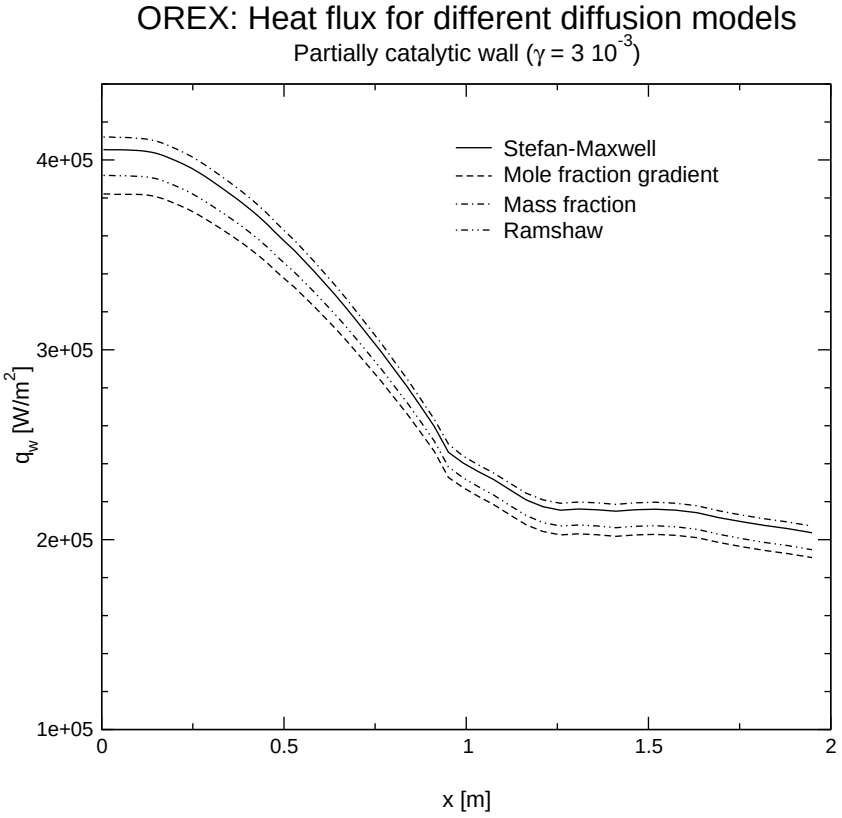

Figure 15: Heat flux for different diffusion models on OREX vehicle

Concerning the computational cost we found out that Fick's law approximation is 25 % faster than Stefan-Maxwell and Ramshaw 14 % faster. From the previous discussion is clear that Fick's law approximation has to be discarded for diffusion modeling, leaving Ramshaw and Stefan-Maxwell as the only acceptable choices. Our suggestion is as follows: Ramshaw formulation is used in the transient phase of the computation to take advantage of the lower cost, Stefan-Maxwell formulation is switched on in the last phase of the computation to converge to the final solution.

References

Anderson, J. D. (1989). *Hypersonic and High Temperature Gas Dynamics*. McGraw-Hill.

Barbante, P. F. (2001). *Accurate and Efficient Modelling of High Temperature Nonequilibrium Air Flows*. PhD thesis, ULB-VKI, Bruxelles, Belgium.

Bottin, B., Vanden Abeele, D., Carbonaro, M., Degrez, G., and Sarma, G. S. R. (1999). Thermodynamic and Transport Properties for Inductive Plasma Modeling. *J. of Thermophysics and Heat Transfer*, 13(3):343–350.

Capitelli, M., Gorse, C., Longo, S., and Giordano, D. (2002). Collision Integrals of High-temperature Air Species. *J. of Thermophysics and Heat Transfer*, 14(2):259–268.

Chapman, S. and Cowling, T. G. (1970). *The Mathematical Theory of Non-Uniform Gases*. Cambridge University Press.

Chase, M. W., Davies, C. A., Downey, J. R., Frurip, D. J., McDonald, R. A., and Syverud, A. (1985). JANAF Thermochemical Tables, Third Ed. Part II, Cr-Zr. *J. of Phys. and Chem.*, 14(suppl. 1).

Clarke, J. F. and McChesney, M. (1964). *The Dynamics of Real Gases*. Butterworths.

Delcroix, J.-L. and Bers, A. (1994). *Physique des plasmas*. Inter Éditions, CNRS Éditions.

Devoto, R. S. (1966). Transport Properties of Ionized Monoatomic Gases. *The Physics of Fluids*, 9(6):1230–1240.

Devoto, R. S. (1967). Simplified Expressions for the Transport Properties of Ionized Monoatomic Gases. *The Physics of Fluids*, 10(10):2105–2112.

Ferziger, J. H. and Kaper, H. G. (1972). *Mathematical Theory of Transport Processes in Gases*. North Holland.

Giovangigli, V. (1999). *Multicomponent Flow Modeling*. Birkhäuser.

Gupta, R. N. (1996a). Two and Three-Dimensional Analysis of Hypersonic Nonequilibrium Low-Density Flows. *J. of Thermophysics and Heat Transfer*, 10(2):267–276.

Gupta, R. N. (1996b). Viscous Shock-Layer Study of Thermochemical Nonequilibrium. *J. of Thermophysics and Heat Transfer*, 10(2):257–266.

Gupta, R. N., Moss, J. N., and Price, J. M. (1996). Assessment of Thermochemical Nonequilibrium and Slip Effects for Orbital Reentry Experiment OREX. AIAA Paper 96-1859.

Gupta, R. N., Yos, J. M., Thompson, R. A., and Lee, K. P. (1990). A Review of Reaction Rates and Thermodynamic and Transport Properties for an 11-Species Air Model for Chemical and Thermal Nonequilibrium Calculations to 30000 K. RP 1232, NASA.

Hirschfelder, J. O., Curtiss, C. F., and Bird, R. B. (1954,1964). *Molecular Theory of Gases and Liquids*. John Wiley & Sons. Second printing, corrected, with notes.

Kurotaki, T. (2000). Construction of Catalytic Model on SiO_2 Based Surface and Application to Real Trajectory. In *AIAA* 34^{th} *Thermophysics Conference*, AIAA Paper 2000-2366.

Magin, T. and Degrez, G. (2004a). Transport Algorithms for Partially Ionized and Unmagnetized Plasmas. *Journal of Computational Physics*. To appear.

Magin, T. and Degrez, G. (2004b). Transport Properties of Partially Ionized and Unmagnetized Plasmas. *Physical Review E*. To appear.

Magin, T., Degrez, G., and Sokolova, I. (2002). Thermodynamics and transport properties of Martian atmosphere for space entry application. In *33rd Plasmadynamics and Lasers Conference*, AIAA Paper 2002-2226.

Mayer, J. E. and Mayer, M. G. (1946). *Statistical Mechanics*. John Wiley & Sons.

Mitchner, M. and Kruger, C. H. (1973). *Partially Ionized Gases*. John Wiley & Sons.

Nasuti, F., Barbato, M., and Bruno, C. (1996). Material-Dependent Catalytic Recombination Modeling for Hypersonic Flows. *J. of Thermophysics and Heat Transfer*, 10(1):131–136.

Park, C. (1990). *Nonequilibrium Hypersonic Aerothermodynamics*. John Wiley & Sons.

Park, C. (1993). Review of Chemical-Kinetics Problems of Future NASA Missions, I: Earth Entries. *J. of Thermophysics and Heat Transfer*, 7(3):385–398.

Peterkin, R. E. and Turchi, P. J. (2000). Magnetohydrodynamics Theory for Hypersonic Plasma Flow: What's Important and What's Not. AIAA Paper 2000-2257.

Ramshaw, J. D. (1990). Self-Consistent Effective Binary Diffusion in Multicomponent Gas Mixtures. *J. of Non-Equilib. Thermodyn.*, 15:295–300.

Reggiani, S., Barbato, M., Bruno, C., and Muylaert, J. (1996). Model for Heterogeneous Catalysis on Metal Surfaces with Applications to Hypersonic Flows. In *AIAA* 31^{st} *Thermophysics Conference*, AIAA Paper 96-1902.

Sarma, G. S. R. (2000). Physico-Chemical Modelling in Hypersonic Flow Simulation. *Progress in Aerospace Sciences*, 36(3-4):281–349.

Sutton, G. W. and Sherman, A. (1965). *Engineering Magnetohydrodynamics*. McGraw-Hill.

Sutton, K. and Gnoffo, P. (1998). Multi-component Diffusion with Application to Computational Aerothermodynamics. In 7^{th} *AIAA/ASME Joint Thermophysics and Heat Transfer Conference*, AIAA Paper 98-2575.

Vincenti, W. G. and Kruger, C. H. (1965). *Introduction to Physical Gas Dynamics*. John Wiley & Sons.

A Transport systems

The transport systems are expressed in terms of binary diffusion coefficients $\mathscr{D}_{ij}$, collision integral ratios $A^\star_{ij}$, $B^\star_{ij}$, $C^\star_{ij}$, $i,j \in \mathcal{H}$, and reduced collision integrals $\bar{Q}^{(1,s)}_{ie}$ $(s = 1,\ldots,5)$, $\bar{Q}^{(2,2)}_{ee}$, $\bar{Q}^{(2,3)}_{ee}$, $\bar{Q}^{(2,4)}_{ee}$ defined by Magin and Degrez (2004a). The kinetic data used to compute the transport coefficients are given by Capitelli et al. (2002) for air and Magin et al. (2002) for carbon dioxide.

• *Heavy-particle subsystem*, $i,j \in \mathcal{H}$

$$G^{\mu}_{ij} = G^{\mu}_{ji} = \frac{1}{T_h} H^{00}_{ij} = \frac{x_i x_j}{n\mathscr{D}_{ij}} \frac{1}{(m_i+m_j)} \left(\frac{6}{5} A^\star_{ij} - 2\right), \; i \neq j, \tag{88a}$$

$$G^{\mu}_{ii} = \frac{1}{T_h} H^{00}_{ii} = \sum_{\substack{j\in\mathcal{H}\\ j\neq i}} \frac{x_i x_j}{n\mathscr{D}_{ij}} \frac{1}{(m_i+m_j)} \left(\frac{6}{5}\frac{m_j}{m_i} A^\star_{ij} + 2\right) + \frac{x_i^2}{\eta_i}, \tag{88b}$$

$$G^{\lambda_h}_{ij} = G^{\lambda_h}_{ji} = \Lambda^{11}_{ij} = \frac{1}{25k_B} \frac{x_i x_j}{n\mathscr{D}_{ij}} \frac{m_i m_j}{(m_i+m_j)^2} \left(16A^\star_{ij} + 12B^\star_{ij} - 55\right), \; i \neq j, \tag{88c}$$

$$G^{\lambda_h}_{ii} = \Lambda^{11}_{ii} = \frac{1}{25k_B} \sum_{\substack{j\in\mathcal{H}\\ j\neq i}} \frac{x_i x_j}{n\mathscr{D}_{ij}} \frac{1}{(m_i+m_j)^2} \left(30m_i^2 + 25m_j^2 - 12m_j^2 B^\star_{ij} + 16m_i m_j A^\star_{ij}\right) + \frac{4}{15k_B} \frac{x_i^2 m_i}{\eta_i}, \tag{88d}$$

$$\Lambda^{01}_{ij} = \Lambda^{10}_{ji} = \frac{1}{25k_B} \frac{x_i x_j}{n\mathscr{D}_{ij}} \frac{m_i}{(m_i+m_j)} \left(12C^\star_{ij} - 10\right), \; i \neq j, \tag{88e}$$

$$\Lambda^{01}_{ii} = \Lambda^{10}_{ii} = -\frac{1}{25k_B} \sum_{\substack{j\in\mathcal{H}\\ j\neq i}} \frac{x_i x_j}{n\mathscr{D}_{ij}} \frac{m_j}{(m_i+m_j)} \left(12C^\star_{ij} - 10\right), \tag{88f}$$

$$\hat{G}^{\vec{V}}_{ij} = \hat{G}^{\vec{V}}_{ji} = -\frac{x_i x_j}{\mathscr{D}_{ij}} \left(1 + \varphi_{ij}\right), \; i \neq j, \tag{88g}$$

$$\hat{G}^{\vec{V}}_{ii} = \sum_{\substack{j\in\mathcal{H}\\ j\neq i}} \frac{x_i x_j}{\mathscr{D}_{ij}} \left(1 + \varphi_{ij}\right). \tag{88h}$$

Correction functions of the Stefan-Maxwell equation are obtained in various Laguerre-Sonine approximations:

$$\sum_{k\in\mathcal{H}} G^{\lambda_h}_{ik} \beta_{kj,1}(2) = -2\Lambda^{01}_{ji}, \; i,j \in \mathcal{H}, \tag{89a}$$

$$\varphi_{ij}(1) = 0, \tag{89b}$$

$$\varphi_{ij}(2) = -\frac{25}{8} n k_B \frac{\mathscr{D}_{ij}}{x_i x_j} \sum_{k\in\mathcal{H}} \Lambda^{01}_{ik} \beta_{kj,1}(2). \tag{89c}$$

• *Heavy-particle electron subsystem*, $i \in \mathcal{H}$

$$\Lambda^{01}_{ie} = \Lambda^{10}_{ei} = -\frac{64 x_e x_i}{75k_B} \frac{T_e}{T_h} \sqrt{\frac{m_e}{2\pi k_B T_e}} \left(\frac{5}{2}\bar{Q}^{(1,1)}_{ie} - 3\bar{Q}^{(1,2)}_{ie}\right), \tag{90a}$$

$$\Lambda^{02}_{ie} = \Lambda^{20}_{ei} = -\frac{64 x_e x_i}{75k_B} \frac{T_e}{T_h} \sqrt{\frac{m_e}{2\pi k_B T_e}} \left(\frac{35}{8}\bar{Q}^{(1,1)}_{ie} - \frac{21}{2}\bar{Q}^{(1,2)}_{ie} + 6\bar{Q}^{(1,3)}_{ie}\right). \tag{90b}$$

- *Electron subsystem*

$$\Lambda_{ee}^{01} = \Lambda_{ee}^{10} = \frac{64x_e}{75k_B}\sqrt{\frac{m_e}{2\pi k_B T_e}}\sum_{j\in\mathcal{H}} x_j\left(\frac{5}{2}\bar{Q}_{ej}^{(1,1)} - 3\bar{Q}_{ej}^{(1,2)}\right), \tag{91a}$$

$$\Lambda_{ee}^{11} = \frac{64x_e}{75k_B}\sqrt{\frac{m_e}{2\pi k_B T_e}}\left[\sum_{j\in\mathcal{H}} x_j\left(\frac{25}{4}\bar{Q}_{ej}^{(1,1)} - 15\bar{Q}_{ej}^{(1,2)} + 12\bar{Q}_{ej}^{(1,3)}\right) + x_e\sqrt{2}\bar{Q}_{ee}^{(2,2)}\right], \tag{91b}$$

$$\Lambda_{ee}^{02} = \Lambda_{ee}^{20} = \frac{64x_e}{75k_B}\sqrt{\frac{m_e}{2\pi k_B T_e}}\sum_{j\in\mathcal{H}} x_j\left(\frac{35}{8}\bar{Q}_{ej}^{(1,1)} - \frac{21}{2}\bar{Q}_{ej}^{(1,2)} + 6\bar{Q}_{ej}^{(1,3)}\right), \tag{91c}$$

$$\Lambda_{ee}^{12} = \Lambda_{ee}^{21} = \frac{64x_e}{75k_B}\sqrt{\frac{m_e}{2\pi k_B T_e}}\left[\sum_{j\in\mathcal{H}} x_j\left(\frac{175}{16}\bar{Q}_{ej}^{(1,1)} - \frac{315}{8}\bar{Q}_{ej}^{(1,2)} + 57\bar{Q}_{ej}^{(1,3)} - 30\bar{Q}_{ej}^{(1,4)}\right) + x_e\sqrt{2}\left(\frac{7}{4}\bar{Q}_{ee}^{(2,2)} - 2\bar{Q}_{ee}^{(2,3)}\right)\right], \tag{91d}$$

$$\Lambda_{ee}^{22} = \frac{64x_e}{75k_B}\sqrt{\frac{m_e}{2\pi k_B T_e}}\left[\sum_{j\in\mathcal{H}} x_j\left(\frac{1225}{64}\bar{Q}_{ej}^{(1,1)} - \frac{735}{8}\bar{Q}_{ej}^{(1,2)} + \frac{399}{2}\bar{Q}_{ej}^{(1,3)} - 210\bar{Q}_{ej}^{(1,4)} + 90\bar{Q}_{ej}^{(1,5)}\right) + x_e\sqrt{2}\left(\frac{77}{16}\bar{Q}_{ee}^{(2,2)} - 7\bar{Q}_{ee}^{(2,3)} + 5\bar{Q}_{ee}^{(2,4)}\right)\right]. \tag{91e}$$